ICGEA 2026

Certificate

OF INVITED SPEAKER

This Certificate is Awarded to

Dyah Erny Herwindiati

Universitas Tarumanagara, Indonesia

who served as Invited Speaker at 2026 The 10th International Conference on Green Energy and Applications (ICGEA 2026), which has been held in Hanoi, Vietnam during March 6-8, 2026.

Conference Committee
ICGEA 2026

IEEE

2026 ICGEA

2026 The 10th International Conference on

GREEN ENERGY AND APPLICATIONS

March 6-8, 2026 HUST Hanoi, Vietnam

Sponsored by

Technically Co-sponsored by

Decline in Water Infiltration in the Ciliwung River Flow: Applications of Machine Learning and Environmental Impacts

Dyah Erny Herwindiati

Faculty of Information Technology,
Universitas Tarumanagara - Indonesia

Discussion in the First Research Period

The Objective of Research

- The objective of this research was to classify and map land cover types, including pervious, semi-pervious, impervious surfaces, and water bodies, to estimate infiltration in the Ciliwung River flow using Sentinel-2 satellite imagery.
- Land cover and infiltration mapping were conducted across 22 sub-districts located along the Ciliwung River in Bogor, Depok, and Jakarta.

Background and Case Study

Ciliwung River and Bogor Regency

- The Ciliwung River begins in the mountains between Mount Gede and Mount Pangrango **in Bogor, West Java**.
- Stretching around 124 kilometers, it flows from the Puncak highlands through Bogor Regency, providing a vital water source Jakarta City

Mount Gede – in Bogor Regency

Mount Pangrango – in Bogor Regency

Bogor Regency is Jakarta's water buffer zone

- **Bogor** Regency has historically served as Jakarta's water buffer zone due to its strategic location, extensive open spaces, and forested areas

- The region is designated for soil and water conservation and serves as the largest supplier of water and clean water to Jakarta and the surrounding areas.

Mount SALAK -BOGOR - WEST JAVA

Change of Green to Impervious Land in Bogor

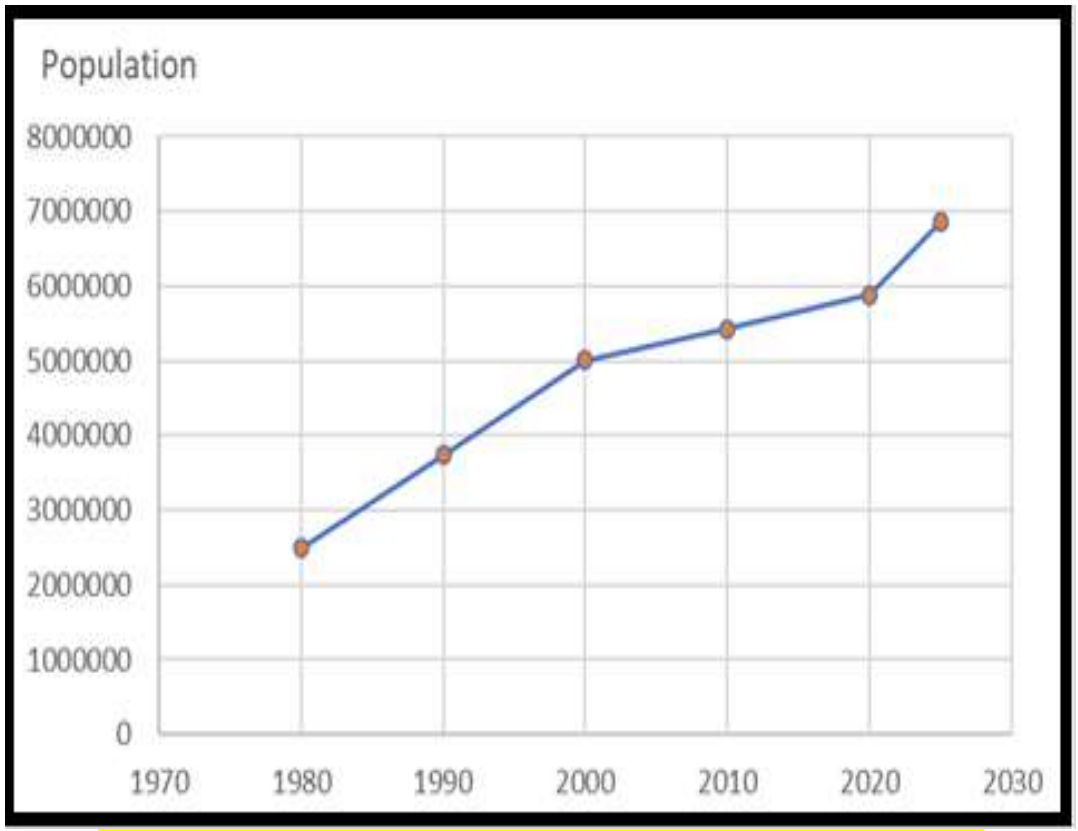

The population in Bogor

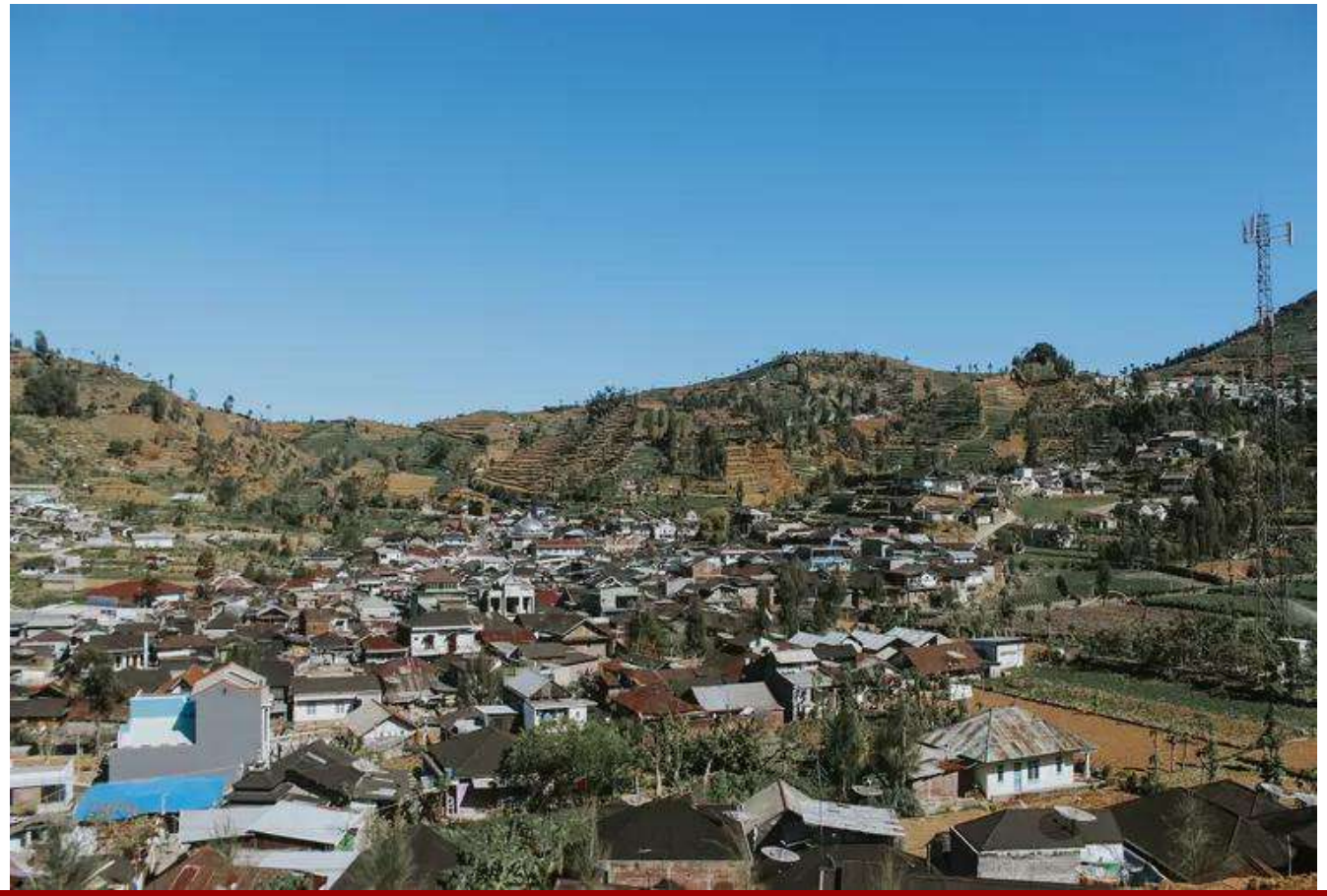

Ciomas Subdistrict - the side of a Salak mountain

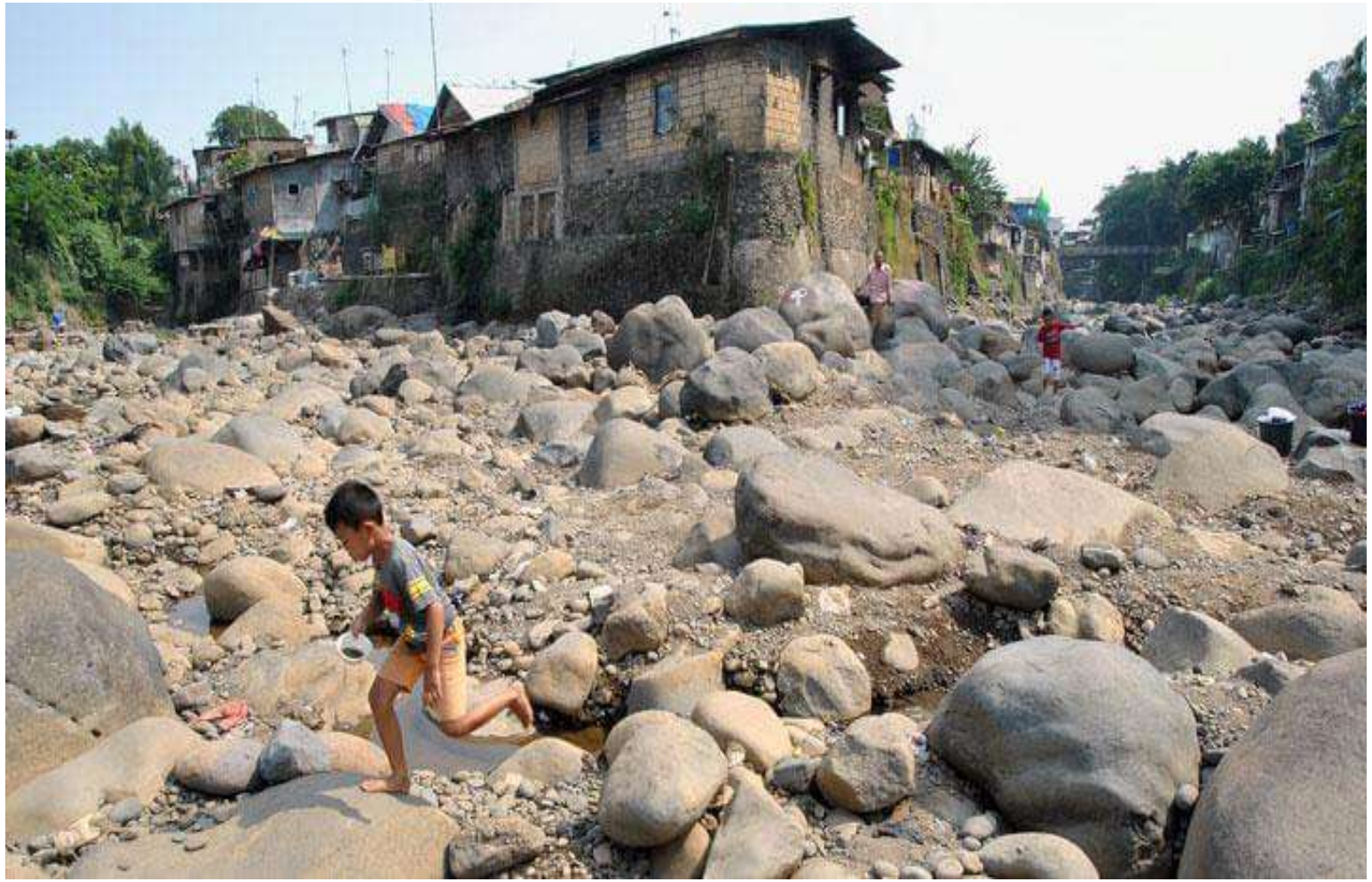

- Bogor is no longer considered a water buffer zone for Jakarta.
- One of the main factors is the rise of residential development. The area can not absorb water maximally

Ciliwung River Flow and Jakarta

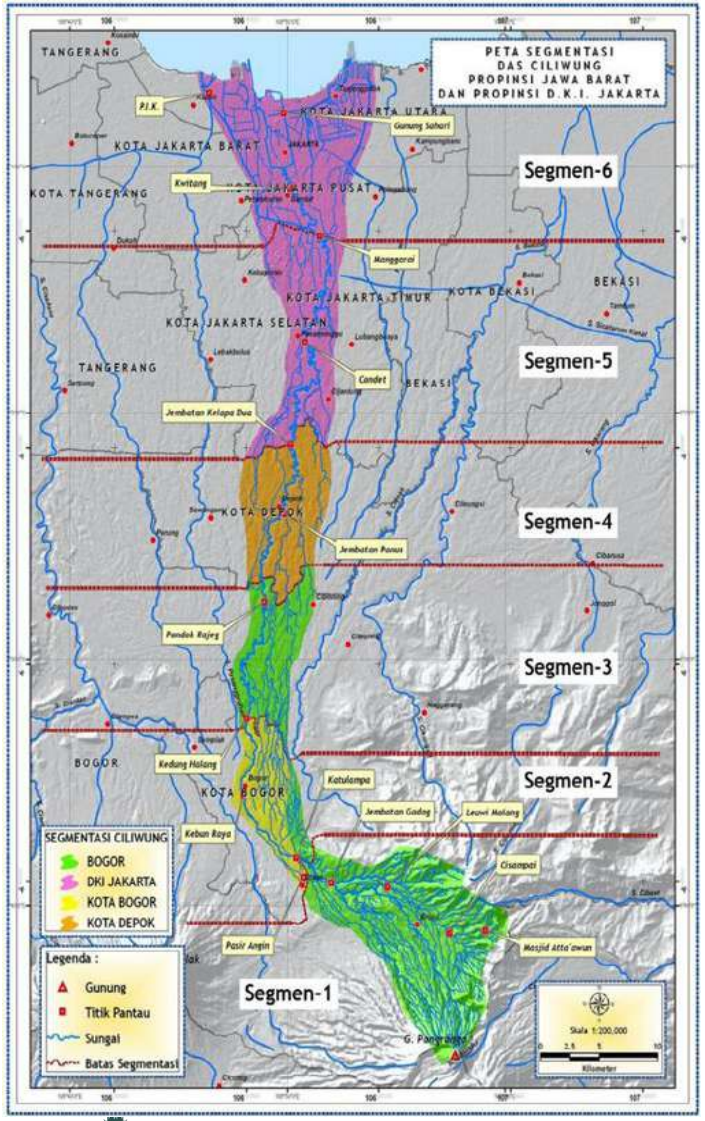

- Jakarta, the capital and largest metropolitan area of Indonesia, serves as the nation's primary economic and financial hub. Over half of Indonesia's monetary transactions take place in Jakarta.
- Jakarta is located along the sixth segment of the Ciliwung River. The river's water is treated to supply clean water to the city. The Ciliwung River is vital for Jakarta's water supply and serves as a main drainage channel, helping to reduce flood risks

The Scope of discussion

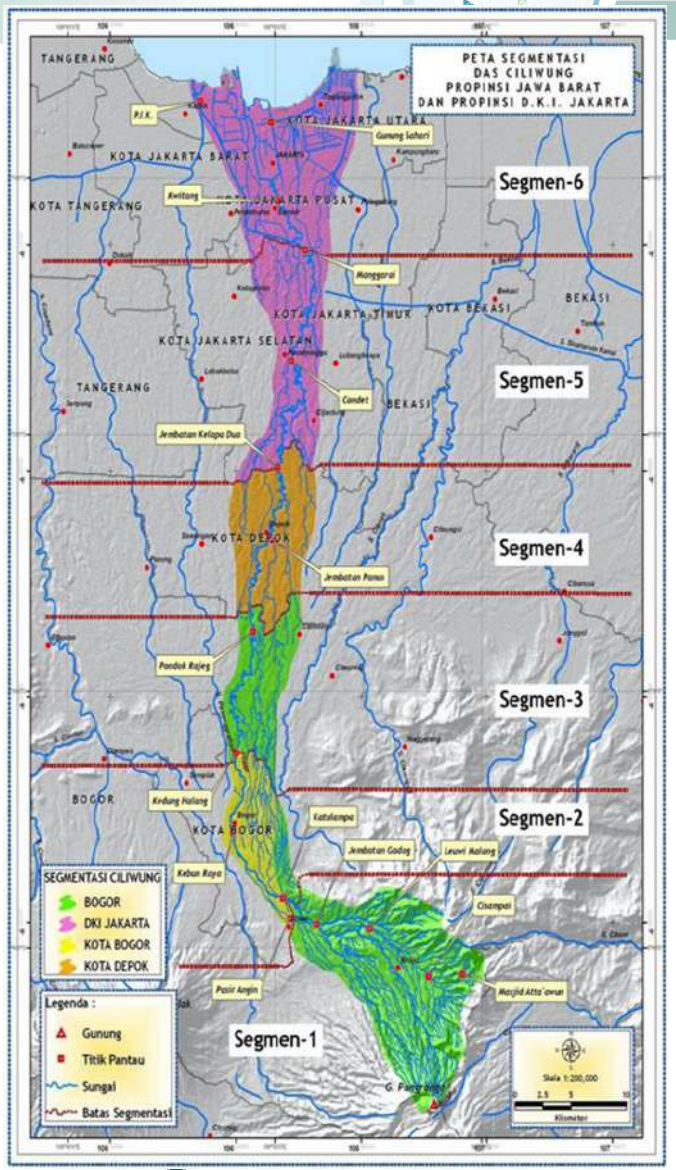

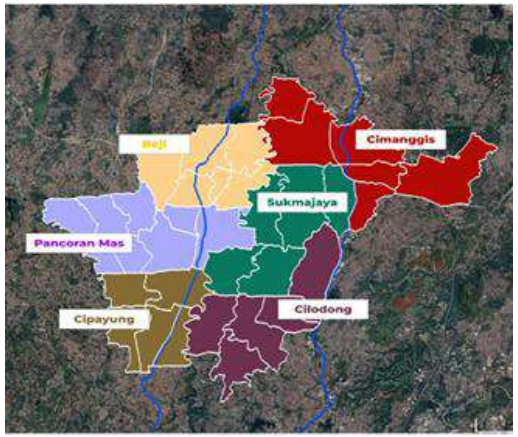

Segment -4
Depok City

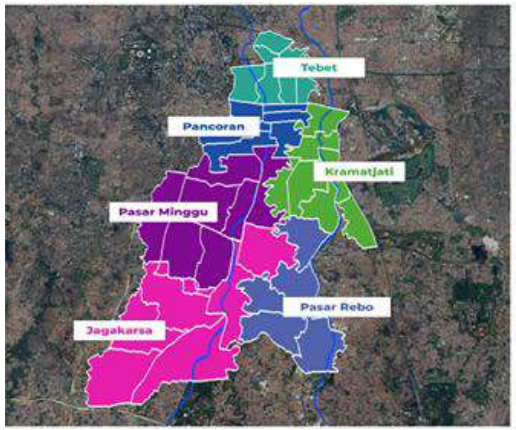

Segment -5
East and South Jakarta

Segment -6
Central Jakarta

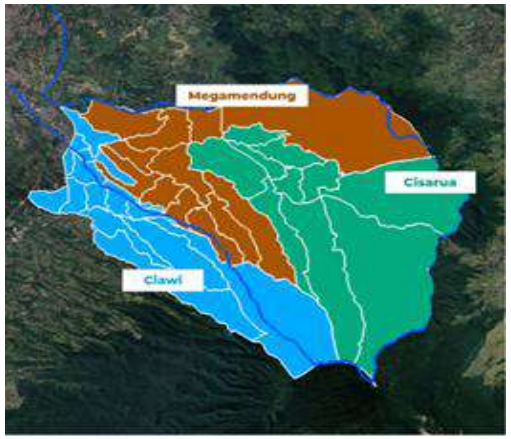

Segment -1
Bogor Regency

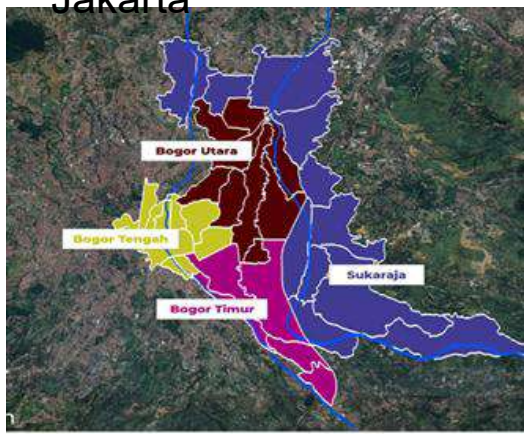

Segment -2
Bogor Regency and City

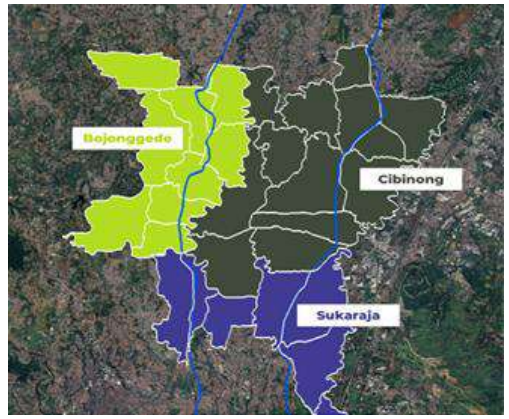

Segment -3
Bogor Regency

The Overall Research Perspective

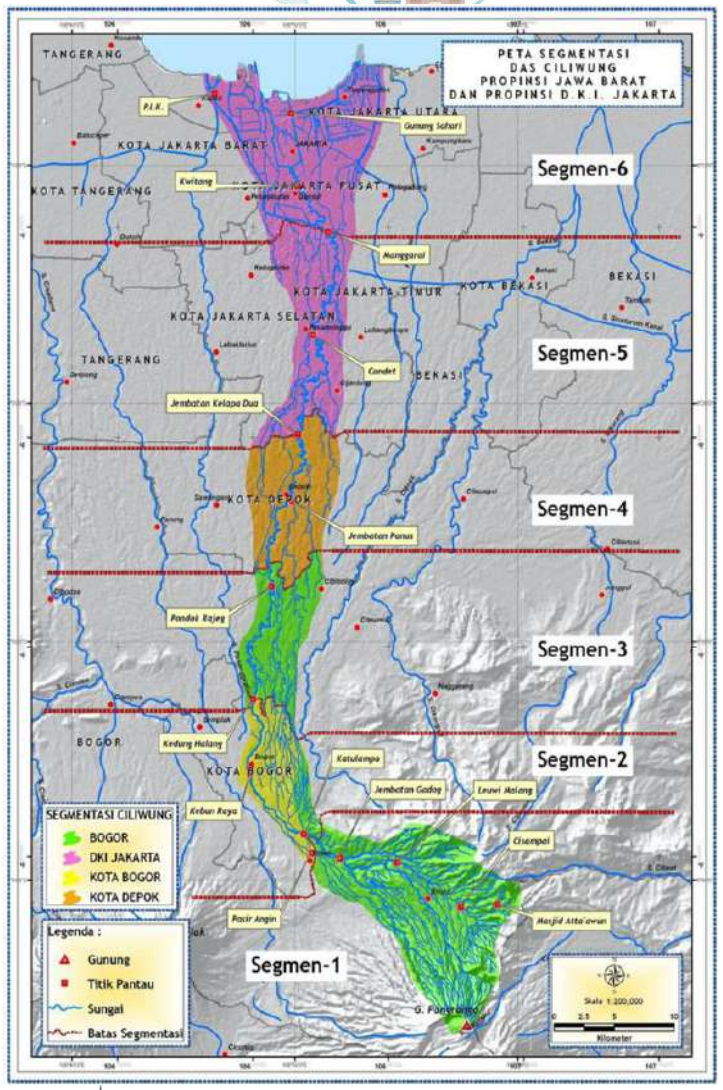

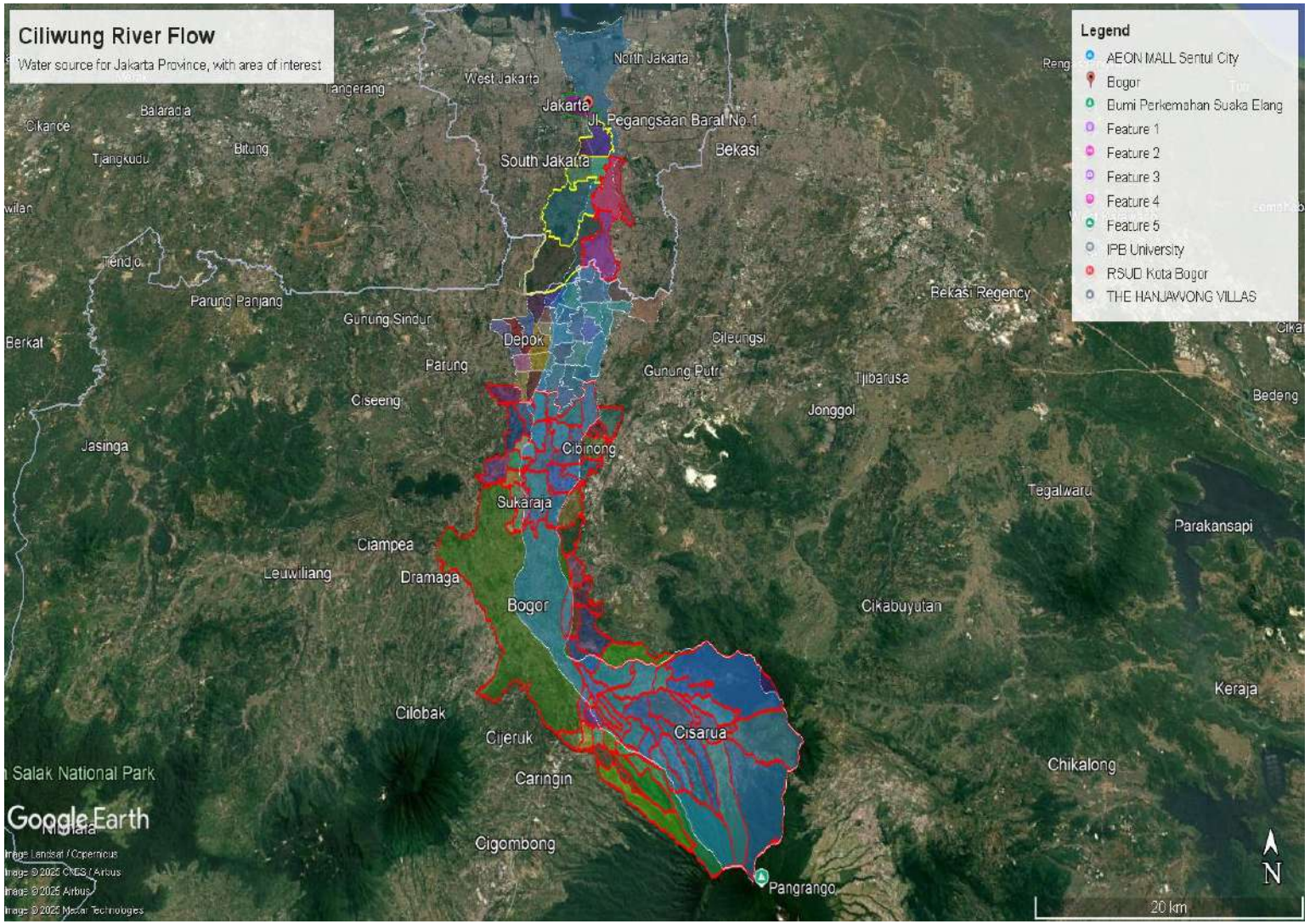

Ciliwung River Flow in Bogor Regency

The Existing Condition in the First and Second Segments

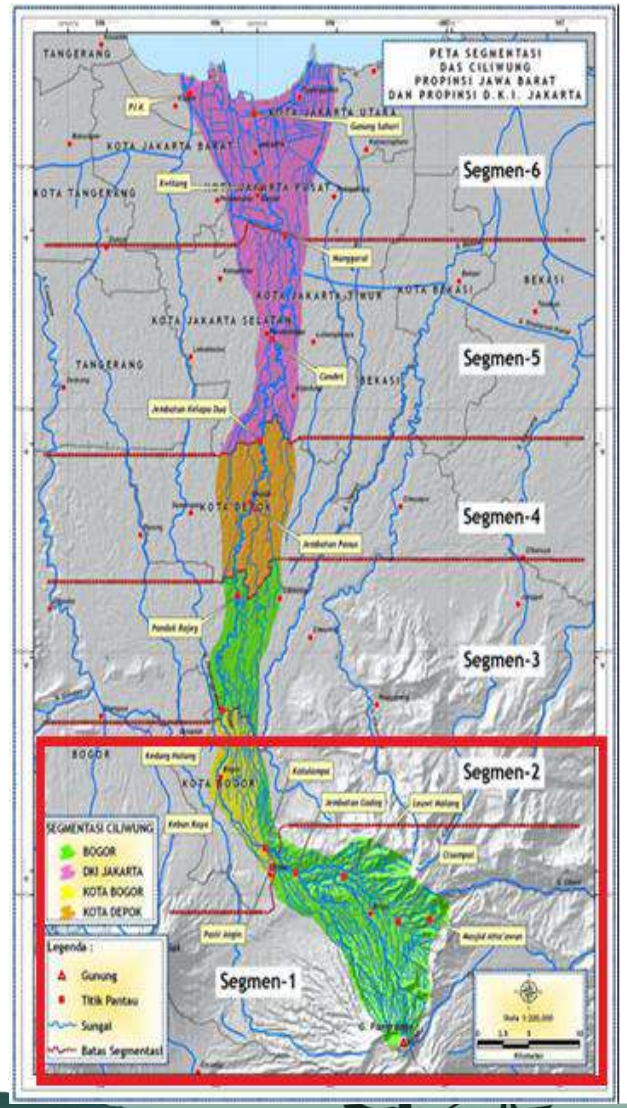

The Second Segment

The First Segment

Ciliwung River Flow in Bogor City

The Existing Condition in The Third Segment

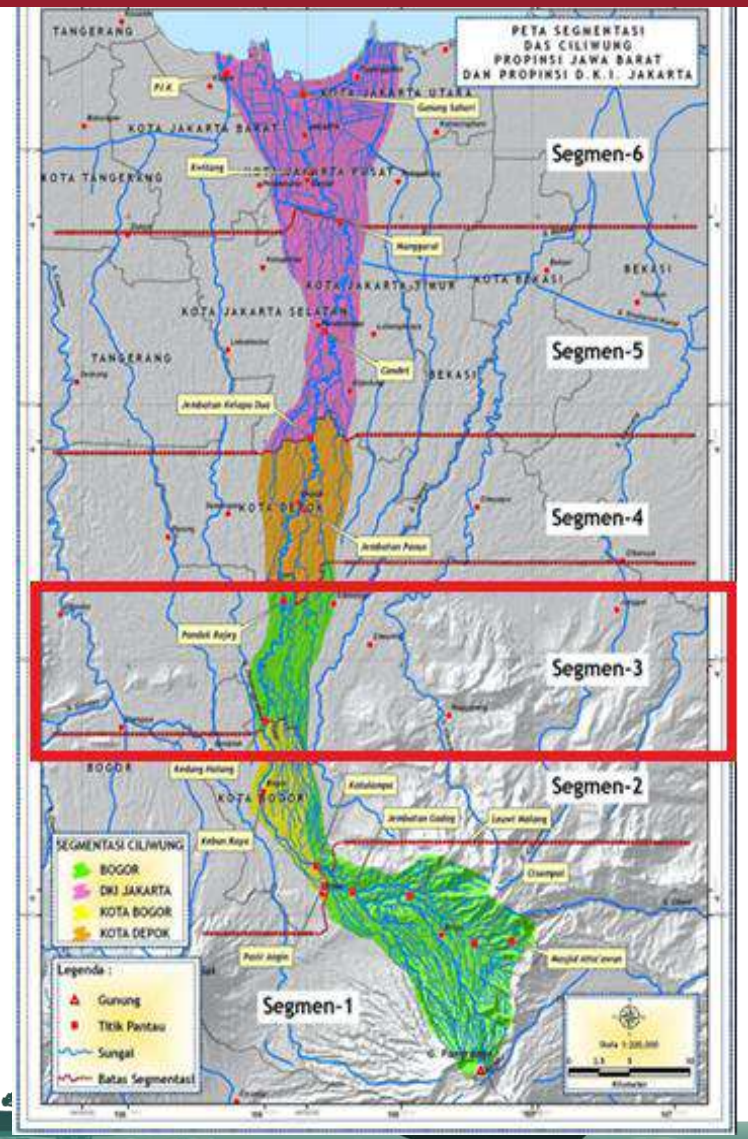

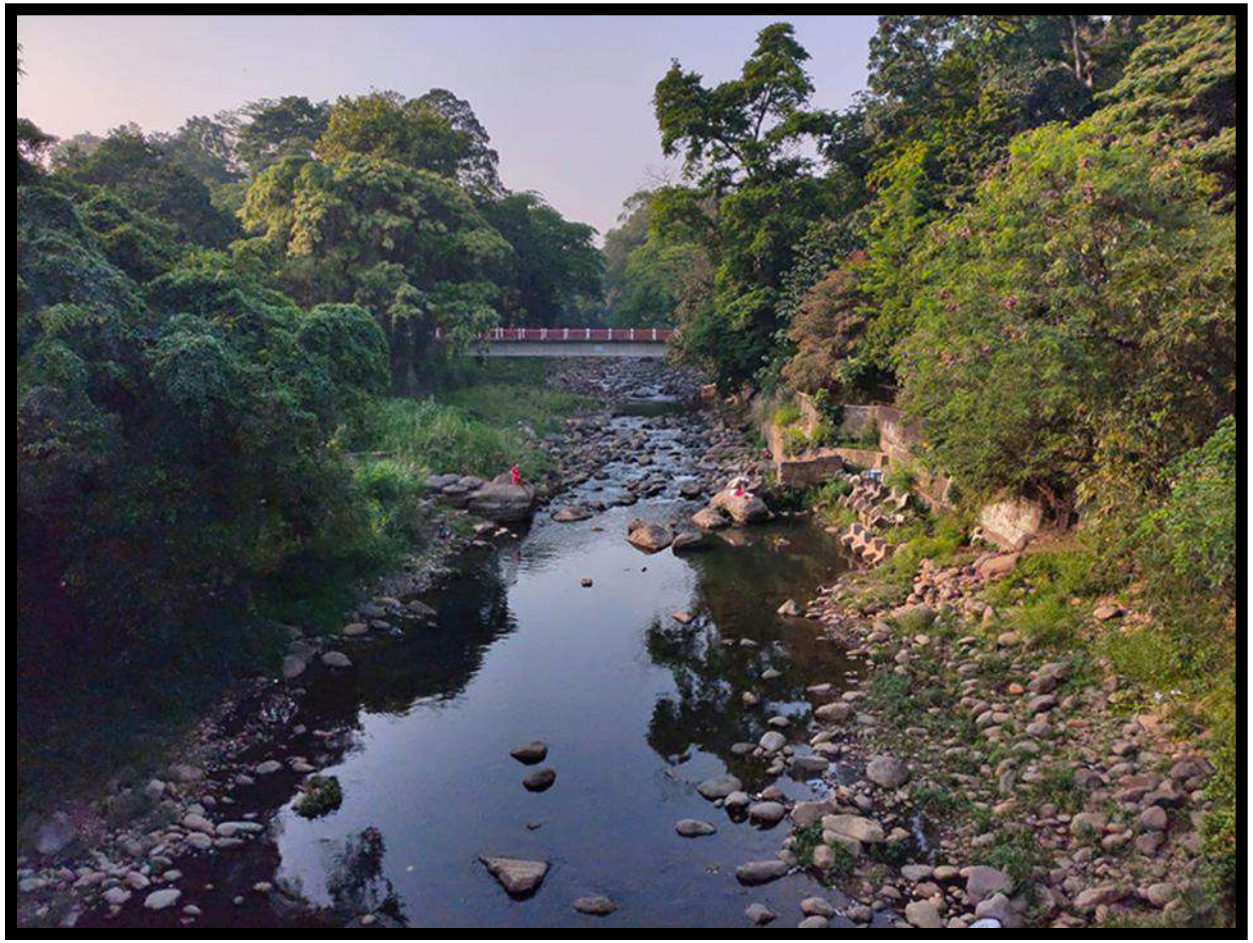

Ciliwung River Flow in Depok City

The Existing Condition in the Fourth Segment

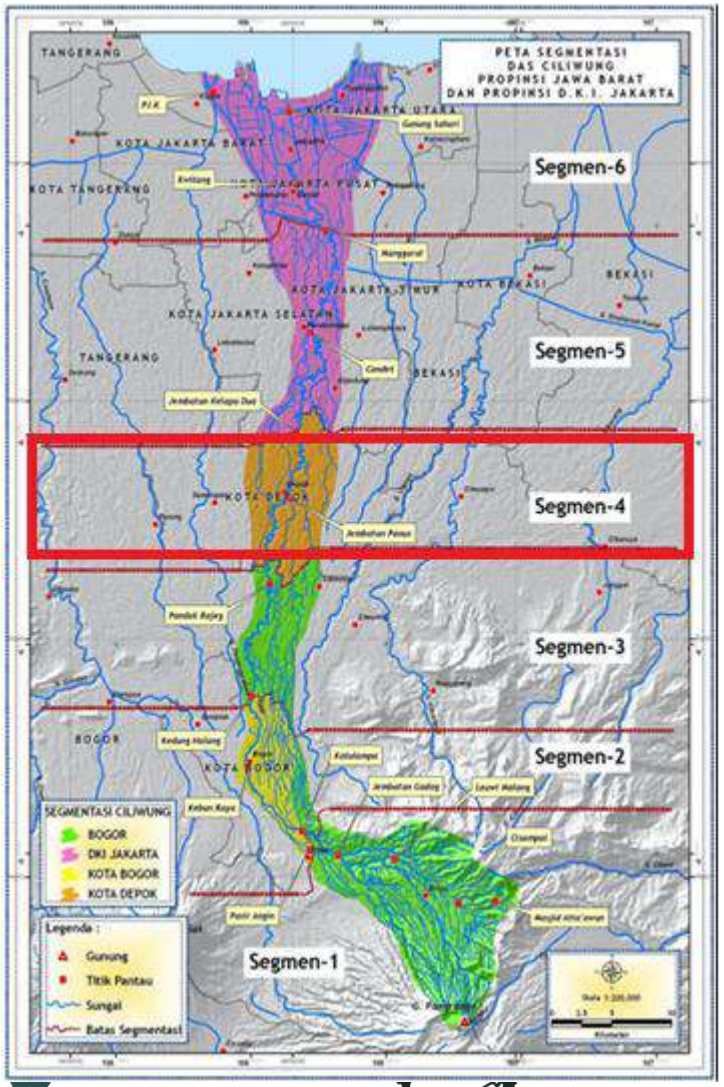

Ciliwung River Flow in Jakarta City

The Existing Condition in the Fifth Segment

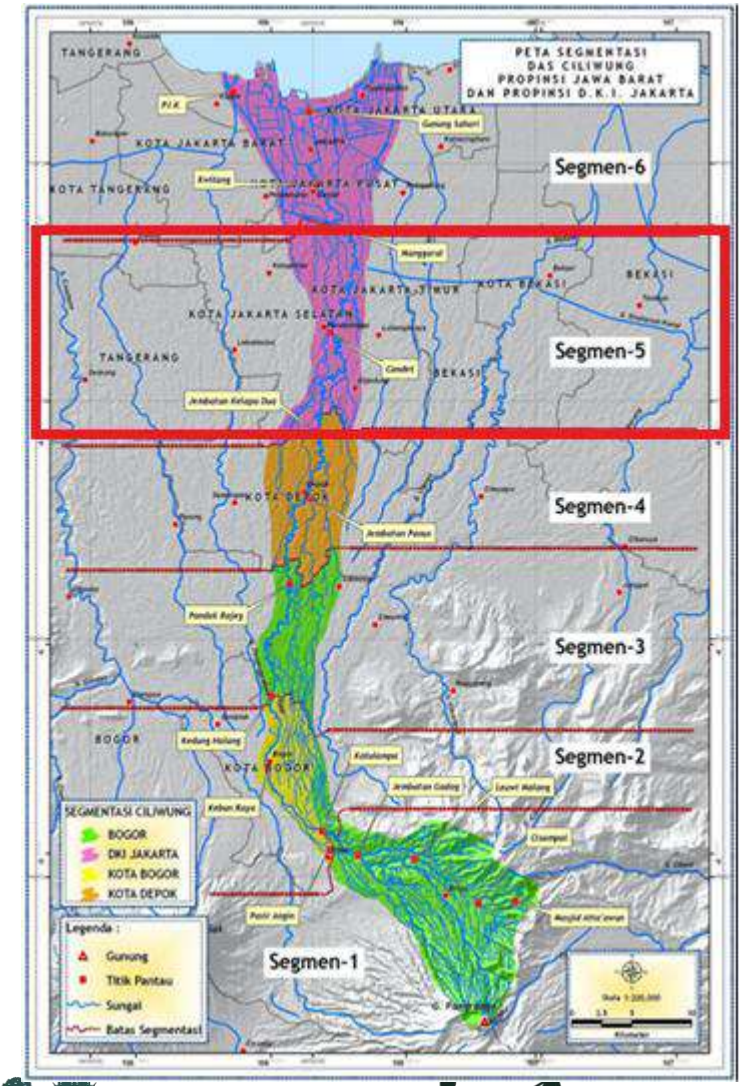

Ciliwung River Flow in Jakarta City

The Existing Condition in the Sixth Segment

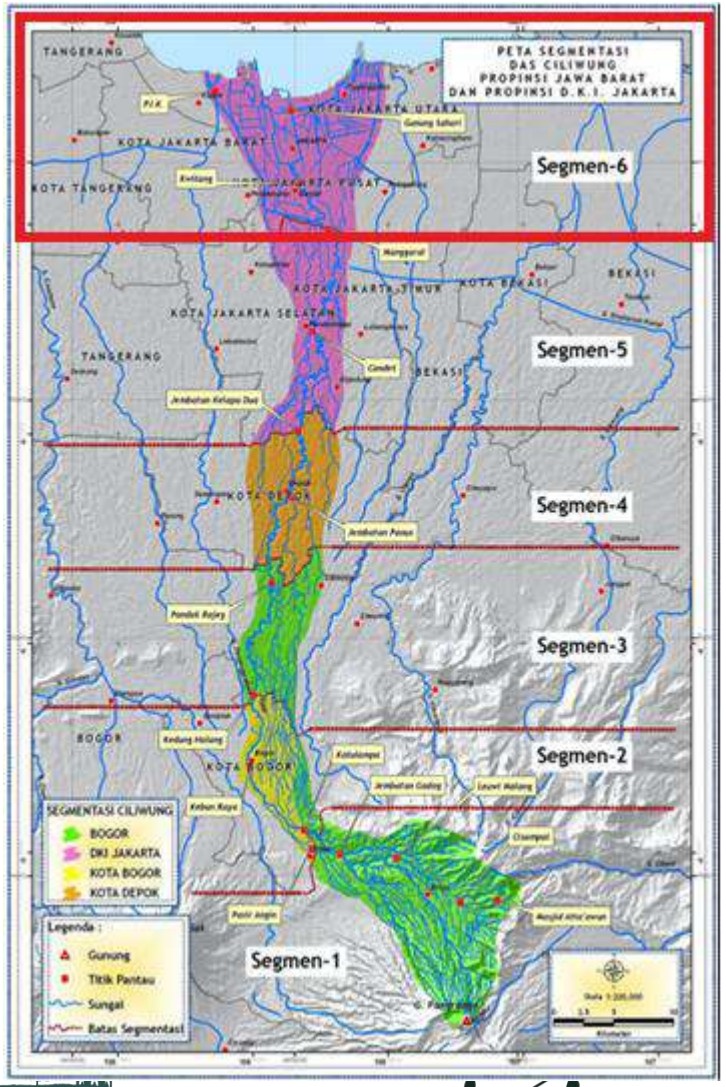

Data Acquisition and Modelling Process

Data Acquisition

- **Sentinel-2 L2A satellite imagery from Copernicus was utilized, with ten spectral bands at 10-meter resolution** selected for surface analysis. The analysis produced thematic maps and numerical statistics.
- **Thematic maps enabled land cover classification into four categories** and facilitated water content estimation using **the Land Surface Water Index (LSWI).**

Remote Sensing: Sentinel-2 Overview

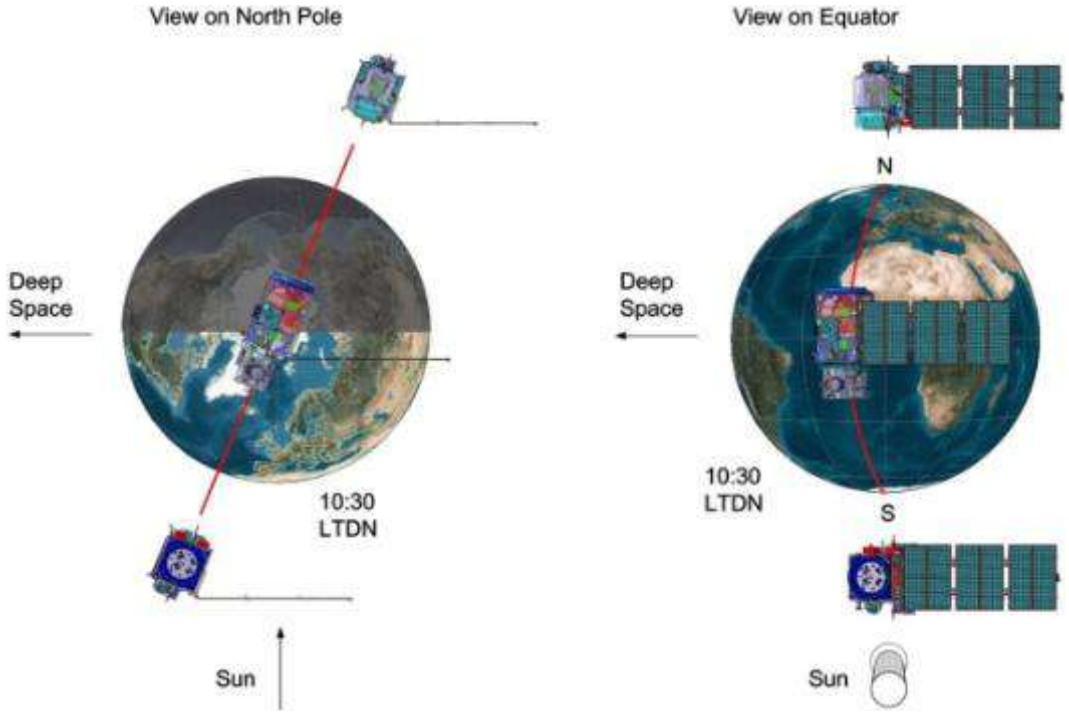

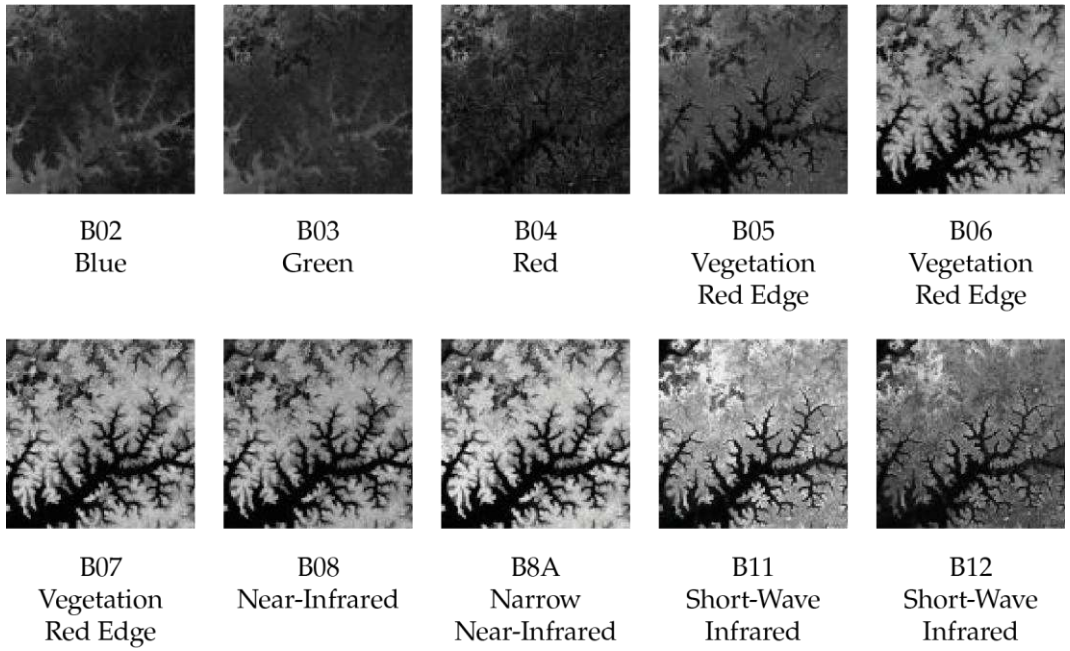

B01: Coastal Aerosol; B09: Water Vapor; B10: Cirrus not included because it is not relevant for analyzing land cover
Source: F. Spoto et al. (2012). Overview of Sentinel-2

UNTAR
Universitas Tarumanagara

Data Acquisition

1. Obtain access tokens for **Copernicus Dataspace by submitting** an HTTP POST request to https://identity.dataspace.copernicus.eu/auth/realms/CDSE/protocol/openid-connect/token.

2. Access the Sentinel-2 data catalog using OData, and download data by referencing the product ID in an HTTP POST request to https://download.dataspace.copernicus.eu/odata/v1/Products($ProductID)/$value.

3. The **acquisition process using an HTTP POST request** returns compressed data in ZIP format. Data are delivered in chunks to accommodate large file sizes.

Data Preview
for Study Area

T48MXU

T48MYU

T48MXT

T48MYT

Data can be acquired for free, either via the Dataspace Browser or through the API for automation.
The tiling system is a slightly modified Military Grid Reference System (MGRS) which is based on the UTM projection.

Land Cover Classification Scheme

Pervious
Natural surface with high permeability, supporting infiltration and groundwater recharge

Impervious
Impermeable surface, does not absorb rainwater, increases runoff

Half-Pervious
Semi-impermeable surface with limited infiltration capacity

Water Body
Surface water bodies, which play a role in water storage and drainage

Pervious, Half Pervious, Impervious Land Cover and A Water Body

- Pervious land cover refers to vegetated surfaces with high permeability that enable rainwater to infiltrate the soil and recharge groundwater.
- Half-pervious land cover partially absorbs water and is commonly found in residential areas with moderate vegetation.
- Impervious land cover refers to surfaces that do not absorb rainwater and are impermeable.
- A water body is a surface that permanently contains water, such as a river, lake, reservoir, or pond. While water bodies have low infiltration, hydrostatic pressure can move water through soil pores, rock cracks, or gaps in the base or walls.

Infiltration

- Infiltration is a vital part of the water cycle, as it determines how much precipitation or surface water penetrates the soil and moves downward through soil pores. This process replenishes soil moisture and groundwater, serving as a key link between surface water and groundwater. Vegetation cover significantly influences infiltration rates.
- Effective infiltration management supports groundwater recharge and helps prevent issues such as waterlogging. High infiltration rates allow rainwater to enter the soil quickly, reducing erosion and minimizing water accumulation that can disrupt mining operations. Conversely, low infiltration rates increase the risk of flooding, as rainwater is not absorbed efficiently.

Vegetation and Water Content

- **Pervious land** is the main support in maintaining **groundwater content**.
- Vegetation shows a **strong linear relationship** with water content through regression analysis.
- Massive **urbanization** in the Ciliwung watershed has **reduced infiltration capacity** and increased the potential for flooding.

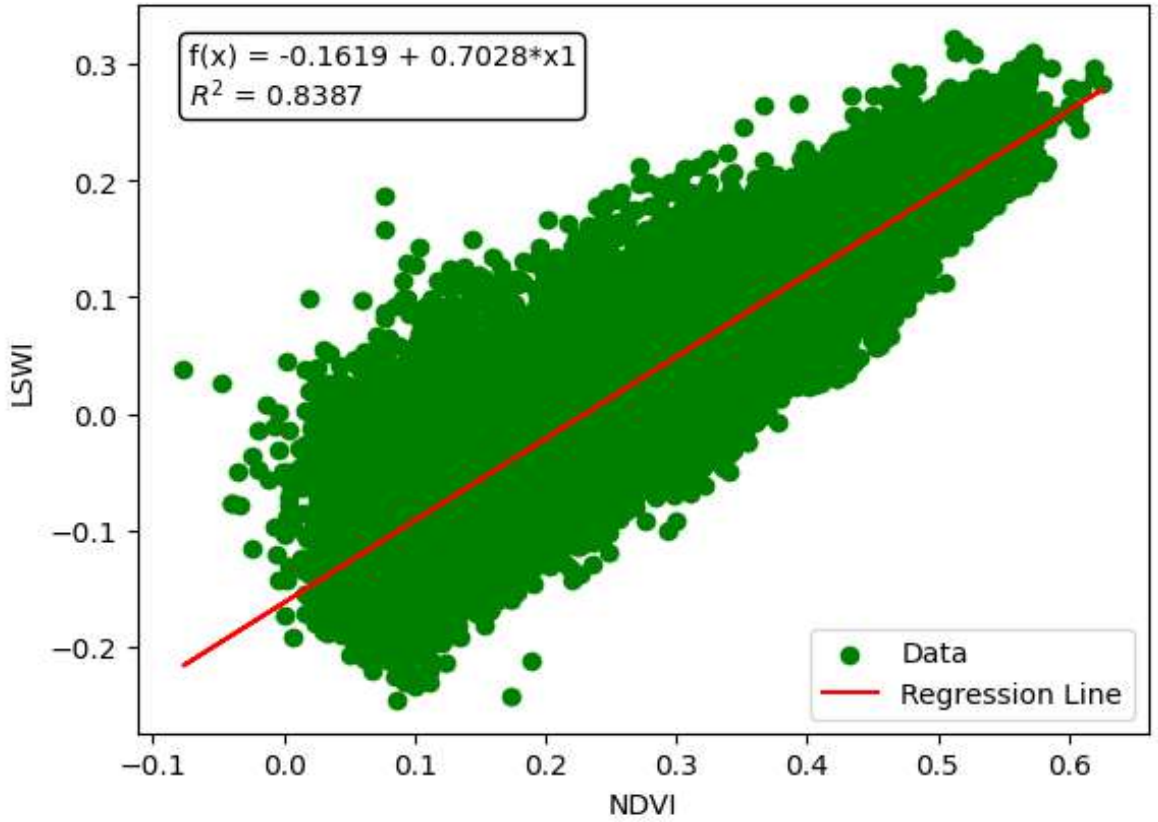

• Normalized Difference Vegetation Index

Higher values indicate dense vegetation, while lower values indicate bare land that tends to be developed or water bodies.

$$NDVI = \frac{\rho_{NIR} - \rho_{Red}}{\rho_{NIR} + \rho_{Red}}$$

• Modified Normalized Difference Water Index

Positive values indicate water bodies, while negative values indicate that the land is not a water body.

$$MNDWI = \frac{\rho_{Green} - \rho_{SWIR1}}{\rho_{Green} + \rho_{SWIR1}}$$

• Enhanced Vegetation Index

Similar to NDVI, but more sensitive to atmospheric disturbance. Directional differences indicate that image pixels have significant disturbance. Used as a validator of data quality.

$$EVI = 2.5 \times \frac{\rho_{NIR} - \rho_{Red}}{\rho_{NIR} + (6 \times \rho_{Red} - 7.5 \times \rho_{Blue}) + 1}$$

• Enhanced Normalized Difference Impervious Surface Index

The more robust for identifying impervious surface based on positive value.

$$ENDISI = \frac{\rho_{Blue} - \alpha \times \left[\frac{\rho_{SWIR1}}{\rho_{SWIR2}} + (MNDWI)^2\right]}{\rho_{Blue} + \alpha \times \left[\frac{\rho_{SWIR1}}{\rho_{SWIR2}} + (MNDWI)^2\right]}$$

$$\alpha = \frac{2 \times (\rho_{Blue})_{Mean}}{\left(\frac{\rho_{SWIR1}}{\rho_{SWIR2}}\right)_{Mean} + [(MNDWI)^2]_{Mean}}$$

• Land Surface Water Index

Measures water saturation, used to estimate water content, with values above 0.2.

$$LSWI = \frac{\rho_{NIR} - \rho_{SWIR}}{\rho_{NIR} + \rho_{SWIR}}$$

The Labelling Process

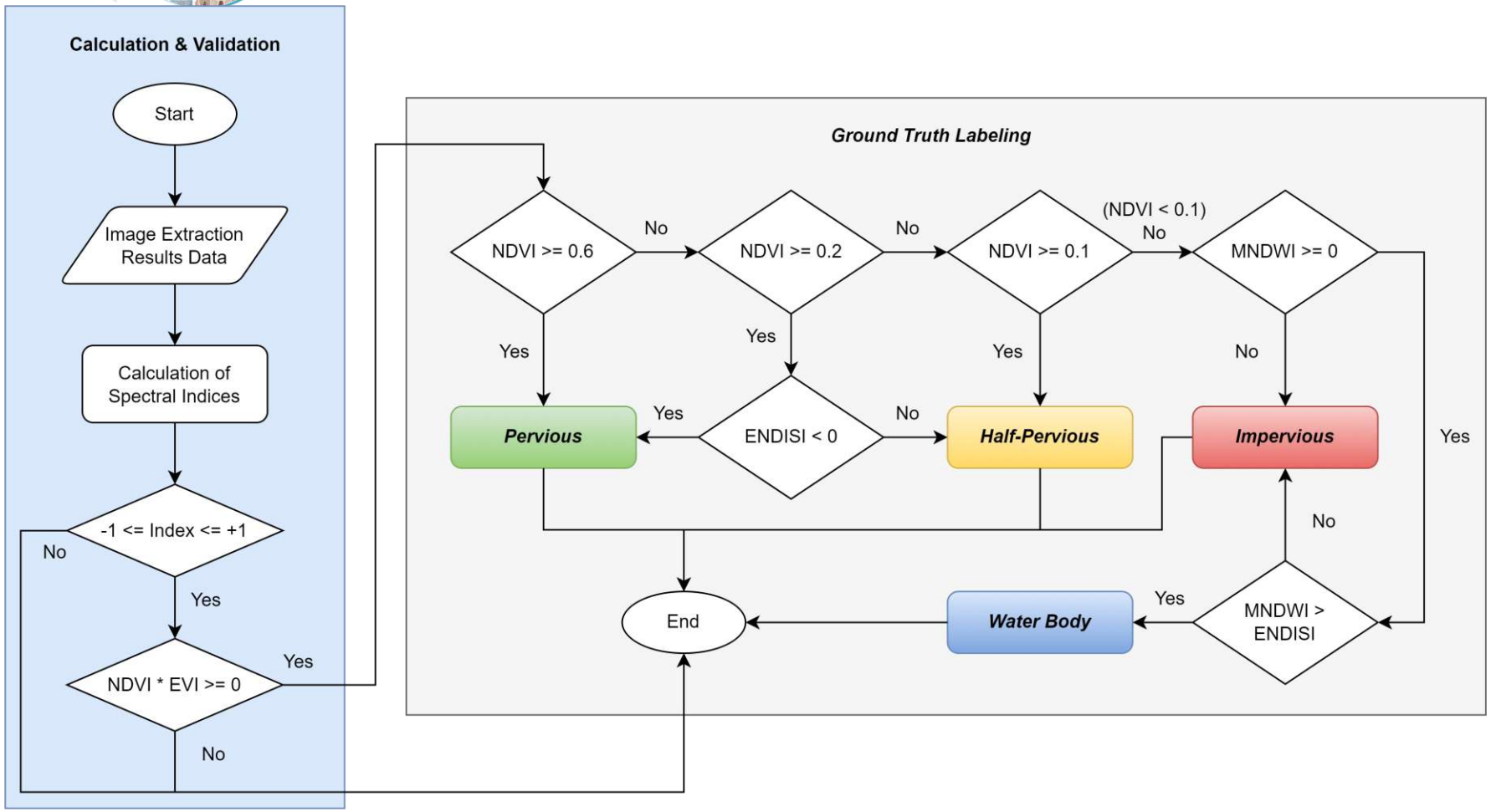

The ground truth labeling scheme was adapted from several previous research in the field of remote sensing, with thresholds used to determine the classification of each land area into a specific class. EVI is the Enhanced Vegetation Index, an index similar to NDVI with the addition of the Blue band as a validator of whether the pixels being observed have significant spectral disturbance.

The Basic Concept of Modelling

One of the most fundamental approaches is **linear regression**, which assumes a linear relationship between the features and the target as follows:

$$y = X\beta + \epsilon$$

Where:

- β is the regression coefficient, which includes: $\beta_1, \beta_2, \ldots, \beta_p$
- ϵ is the residual

The parameters β are generally estimated using the **Ordinary Least Squares (OLS)** method with the following formulation:

$$\beta = (X'X)^{-1}X'y$$

The Basic Concept of Modelling

When predictors are highly correlated, the $X'X$ matrix becomes nearly singular, leading to unstable and inflated coefficient estimates known as **multicollinearity**. To address this, **Hoerl & Kennard (1970)** proposed **ridge regression**, which stabilizes the model by adding an L_2 penalty to the sum-of-squares loss function, as expressed in the following equation:

$$\mathcal{L}_{ridge}(\beta;\lambda) = \left|\left|Y - X\beta\right|\right|^2 + \lambda \left|\left|\beta\right|\right|^2 = \sum_{i=1}^{n}(Y_i - X_i * \beta)^2 + \lambda \sum_{j=1}^{p} B_j^2$$

Where λ is the regularization parameter that controls the penalty magnitude, ≥ 0

The Basic Concept of Modelling

To prove that the ridge regression estimator truly minimizes the ridge loss function, the first-order derivative of the function with respect to β can be calculated as follows:

$$\frac{\partial}{\partial \beta}\mathcal{L}_{ridge}(\beta;\lambda) = -2X'(Y - X\beta) + 2\lambda I\beta = -2X'Y + 2(X'X + \lambda I)\beta$$

By setting the first-order derivative with respect to β with zero, the ridge regression estimator is obtained as a stationary point of the ridge loss function. This point constitutes a minimum if the Hessian matrix, representing the second-order partial derivative, is positive definite, as formulated below:

$$\frac{\partial^2}{\partial \beta \partial \beta'}\mathcal{L}_{ridge}(\beta;\lambda) = 2(X'X + \lambda I)$$

Where:

- I is Identity matrix of the same dimensions as $X'X$, which is $p\ x\ p$
- λI is the diagonal matrix with λ values along the main diagonal

The Basic Concept of Modelling

The optimal solution of the objective function minimization in ridge regression yields the estimated value of β as follows:

$$\beta = (X'X + \lambda I)^{-1}X'y$$

Kernel-based approaches utilize a real-valued function with two arguments, $k = (x, x') \in \mathbb{R}$ which maps a pair of objects into a value representing the degree of similarity between them. In general, kernel functions are symmetric, $k(x, x') = k(x', x)$.

One of the most popular kernels is the Radial Basis Function (RBF) or Gaussian kernel, which is defined as follows:

$$k(x, x') = \exp(-\gamma\left|\left|x - x'\right|\right|^2)$$

The Basic Concept of Modelling

The optimal ridge regression solution in the primal form is defined in the previous equation. However, this solution is not yet in an inner product form that allows for the application of the **kernel trick**. By utilizing the **matrix inversion lemma**, the solution can be rewritten in the dual form as follows:

$$\beta = X'(XX' + \lambda I)^{-1}y$$

β is the weight vector representing the model coefficients in the original feature space, which hereafter will be referred to as ω.

$$\alpha = (K + \lambda I)^{-1}y$$

Where K is the kernel matrix between pairs of training data

The Basic Concept of Modelling

With the dual coefficient α, the weight vector ω can be represented as a linear combination of the training data, as follows

$$\omega = X'\alpha = \sum_{i=1}^{N} \alpha_i x_i$$

Consequently, the prediction for a new data point x is computed simply by using the kernel function between x and the training data, as defined below:

$$f(x) = \omega'\phi(x) = \sum_{i=1}^{N} \alpha_i k(x, x_i)$$

Multi-Class Classification Model Training

- The model is trained using the **One-vs-Rest** scheme, so that submodels will be formed according to the number of class defined.

$$f(x) = \arg \max_{j \in \{1,\ldots,K\}} f_j(x)$$

- The classification results will be determined based on the above decision function.

Kernel Ridge Regression, *which is essentially a model for regression, used as* ***multi-class classification*** *by changing the ground truth label into a dependent variable constructed in the form of a* ***limited multi-dependent variable***.

Land Cover Class	Y_1	Y_2	Y_3	Y_4
Pervious	1	0	0	0
⋮	⋮	⋮	⋮	⋮
Half – Pervious	0	1	0	0
⋮	⋮	⋮	⋮	⋮
Impervious	0	0	1	0
⋮	⋮	⋮	⋮	⋮
Water Body	0	0	0	1

Y_1 to Y_4 are the dependent variables for training the pervious, half-pervious, impervious, and water body submodels, respectively.

Trained Model Information

Regression Equation

$$f(x) = \sum_{i=1}^{n} \alpha_i K(x_i, x)$$

- $f(x)$: predicted output for the input x
- $K(x_i, x)$: kernel function between the training sample x_i and the test input x
- α_i: coefficient obtained from the model training process
- n: total number of training samples

Performance | Train Data | Dual Coefficients

	SM-P	SM-HP	SM-I	SM-WB
1	-4.8881	8.1593	-4.7552	5.4691
2	0.074	11.9928	3.6461	0.0904
3	3.9981	-1.4297	0.6242	0.2493
4	-0.038	-2.106	3.3092	2.3806
5	-8.3396	-6.4425	1.3758	-0.6988
6	0.5421	-5.2615	23.6047	-0.2169
7	3.4661	-2.5933	-59.4944	-0.5549
8	-0.633	9.4769	29.2719	-3.2614
9	1.8094	26.6174	-5.5759	1.0533
10	2.6978	-1.0945	-35.5029	-0.0848

*Please note that the data displayed is **not the entire dataset**, but only the **top 500 rows**. The SM column shows the submodel and codes P, HP, I, and WB, which stand for pervious, half-pervious, impervious, and water body, respectively.*

Trained Model Information

Dual Form Solution

$$\boldsymbol{\alpha} = (K + \lambda I)^{-1}\mathbf{y}$$

- K: kernel matrix ($n \times n$) with elements $K_{ij} = K(x_i, x_j)$
- λ: L2 regularization parameter (ridge), in this model the value of λ = **0.01**
- I: identity matrix
- $\mathbf{y}$: target vector of the training data

RBF Kernel Function

$$K(x_i, x_j) = \exp(-\gamma \|x_i - x_j\|^2)$$

- x_i and x_j: training samples or with test data
- γ: kernel parameter that controls the width of the Gaussian function, in this model the value of γ = **50**

Model was trained with **75:25** train-test ratio.

Performance | Train Data | Dual Coefficients

	SM-P	SM-HP	SM-I	SM-WB
1	-4.8881	8.1593	-4.7552	5.4691
2	0.074	11.9928	3.6461	0.0904
3	3.9981	-1.4297	0.6242	0.2493
4	-0.038	-2.106	3.3092	2.3806
5	-8.3396	-6.4425	1.3758	-0.6988
6	0.5421	-5.2615	23.6047	-0.2169
7	3.4661	-2.5933	-59.4944	-0.5549
8	-0.633	9.4769	29.2719	-3.2614
9	1.8094	26.6174	-5.5759	1.0533
10	2.6978	-1.0945	-35.5029	-0.0848

*Please note that the data displayed is **not the entire dataset**, but only the **top 500 rows**. The SM column shows the submodel and codes P, HP, I, and WB, which stand for pervious, half-pervious, impervious, and water body, respectively.*

The experiments of Training Model

This study assesses how different sample sizes and Train-Test Ratios affect model performance to identify the most effective classification configuration. The experiments were conducted incrementally, as shown in the table below.

Samples Size per Class	Train-Test Ratio (%)
500; 5,000; 10,000; 12,500; 15,000	50:50, 55:45, 60:40, 65:35, 70:30, 75:25, 80:20

The following slides will provide a detailed breakdown of the classification results for each sample size category.

The experiments of Training Model

At this stage, the model is highly unstable, with a standard deviation of 0.045. The average F1-Score ranges from 0.76 to 0.80, suggesting the model is too sensitive to individual data points. This indicates the dataset is insufficient to capture the full spectral diversity of land cover classes.

Samples Size per Class	Train-Test Ratio	F1-Score	
		Average	Std Dev
500	50:50	0.760745	0.031172
	55:45	0.802957	0.043687
	60:40	0.776142	0.038985
	65:35	0.769022	0.04198
	70:30	0.767295	0.045161
	75:25	0.776338	0.018537
	80:20	0.777851	0.034311

The experiments of Training Model

Increasing the sample size to 5,000 represents a significant turning point, as the model begins to recognize core spectral patterns, and the F1-score ranges from 0.83 to 0.84. The notable decline in standard deviation (from 0.012 to 0.007) demonstrates improved consistency and indicates that the data volume has reached scientific viability.

Samples Size per Class	Train-Test Ratio	F1-Score	
		Average	Std Dev
5,000	50:50	0.832252	0.00983
	55:45	0.840576	0.009106
	60:40	0.834352	0.012622
	65:35	0.838094	0.010752
	70:30	0.829098	0.011775
	75:25	0.836397	0.007036
	80:20	0.84241	0.010485

The experiments of Training Model

Using 10,000 samples, the model effectively captures the spectral signatures of each class. The average F1-Score ranges from 0.840 to 0.850, with a standard deviation below 0.01. These findings indicate that the model has reached a knowledge threshold, providing sufficient data to represent typical land-cover variations.

Samples Size per Class	Train-Test Ratio	F1-Score	
		Average	Std Dev
10,000	50:50	0.840405	0.004672
	55:45	0.841567	0.008008
	60:40	0.845589	0.009457
	65:35	0.845303	0.006797
	70:30	0.846688	0.006022
	75:25	0.848909	0.004717
	80:20	0.850219	0.005544

The experiments of Training Model

When 15,000 samples per class are used, the model attains peak performance and informational saturation, achieving an F1-Score of up to 0.856. This configuration yields the lowest standard deviation (0.0039), which indicates highly consistent results across different data splits. Consequently, a 75:25 train-test ratio with this sample size was selected as the optimal configuration.

Samples Size per Class	Train-Test Ratio	F1-Score	
		Average	Std Dev
15,000	50:50	0.852862	0.005751
	55:45	0.85255	0.006323
	60:40	0.852253	0.00511
	65:35	0.855827	0.006453
	70:30	0.85432	0.004481
	75:25	0.85684	0.004119
	80:20	0.855854	0.003959

With the optimal data configuration established at 15,000 samples per class and a 75:25 train-test ratio, the study proceeded to fine-tune the model's internal architecture. We performed a grid search to optimize the Kernel Ridge Regression (KRR) hyperparameters, specifically the regularization (λ) and the RBF kernel parameter (γ) as shown in the table below:

λ	γ
0.01, 0.05, 0.1, 0.5	10, 20, 50

The detailed performance results for these parameter combinations are presented in the following slide.

λ	γ	F1-Score (KRR)	
		Average	Std Dev
0.01	10	0.960721	0.003
	20	0.966662	0.002289
	50	0.975119	0.002818
0.05	10	0.956025	0.003142
	20	0.962644	0.002421
	50	0.972584	0.002821
0.1	10	0.95339	0.00284
	20	0.96058	0.002566
	50	0.970799	0.002844
0.5	10	0.945253	0.002858
	20	0.955111	0.003067
	50	0.964961	0.003428

Among the tested combinations, the pair of $\lambda = 0.01$ and $\gamma = 50$ was identified as the most effective configuration.

Multi-Class Classification Model Training

- The model is trained using the **One-vs-Rest** scheme, so that submodels will be formed according to the number of class defined.

$$f(x) = \arg \max_{j \in \{1,\ldots,K\}} f_j(x)$$

- The classification results will be determined based on the above decision function.

***Kernel Ridge Regression**, which is essentially a model for regression, used as **multi-class classification** by changing the ground truth label into a dependent variable constructed in the form of a **limited multi-dependent variable**.*

Land Cover Class	Y_1	Y_2	Y_3	Y_4
Pervious	1	0	0	0
⋮	⋮	⋮	⋮	⋮
Half-Pervious	0	1	0	0
⋮	⋮	⋮	⋮	⋮
Impervious	0	0	1	0
⋮	⋮	⋮	⋮	⋮
Water Body	0	0	0	1

Y_1 to Y_4 are the dependent variables for training the pervious, half-pervious, impervious, and water body submodels, respectively.

Trained Model Information

Regression Equation

$$f(x) = \sum_{i=1}^{n} \alpha_i K(x_i, x)$$

Land Cover Class	Precision	Recall	F1-Score
Pervious	0.999172	0.965333	0.981961
Half-Pervious	0.94314	0.964267	0.953586
Impervious	0.966178	0.967467	0.966822
Water Body	0.988648	0.998667	0.993632

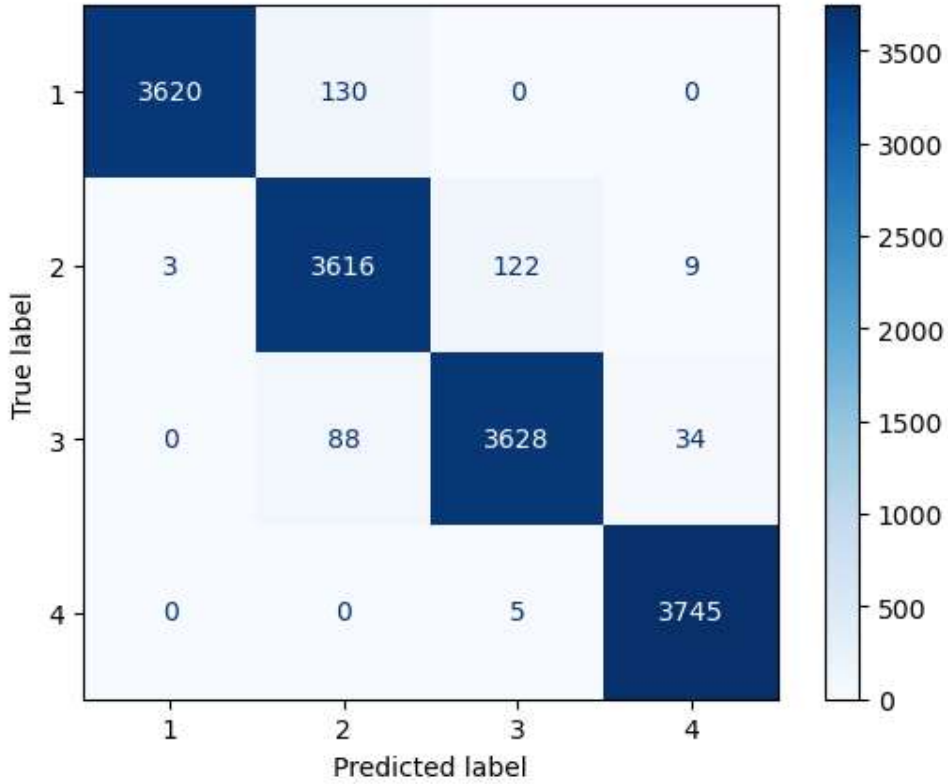

Validation of Model Results

NIR Band *of Sentinel-2 Imagery*

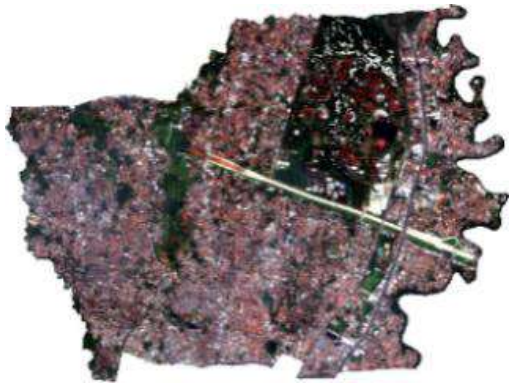

True Color Composite *(RGB)*

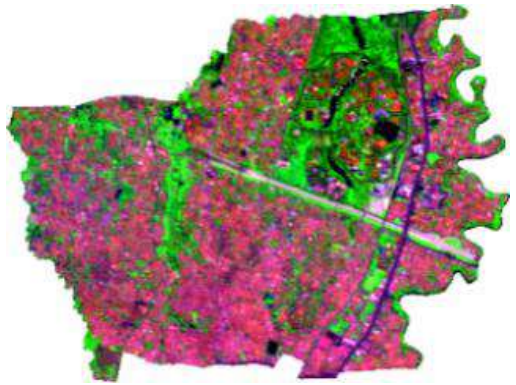

False Color Composite *(SWIR2, NIR, Blue)*

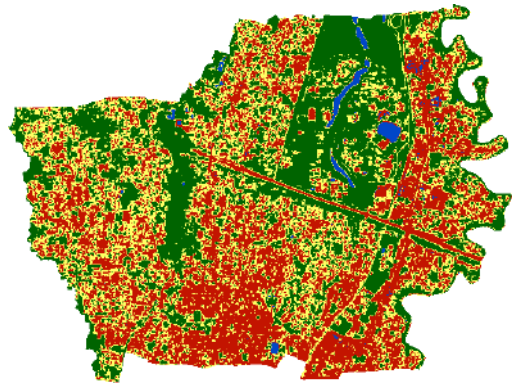

Land Cover Classification Map *generated by the model*

The classification performance of the model will be evaluated using metrics derived from the confusion matrix, and also compared with actual images to see the real conditions. True and false color composites are used to facilitate comparison and validation, as they show the differences for each land type.

The Mapping of Land Cover

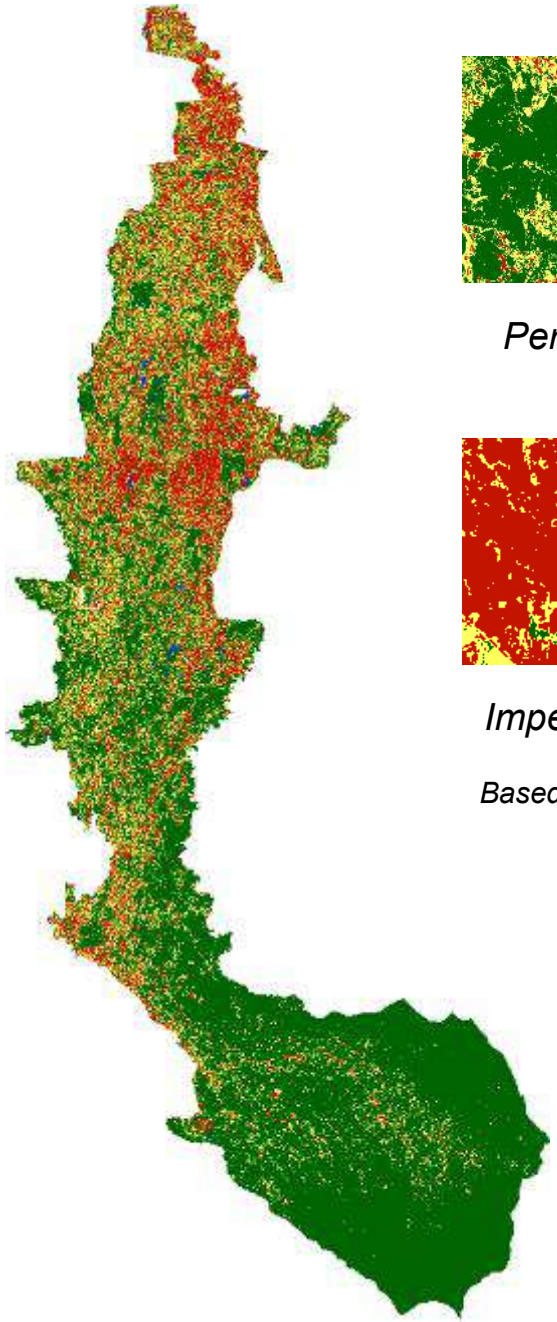

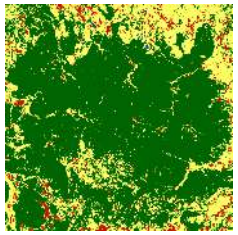

Pervious

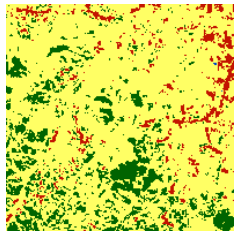

Half-Pervious

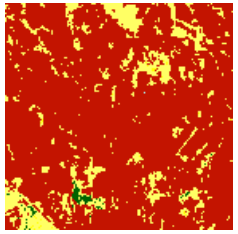

Impervious

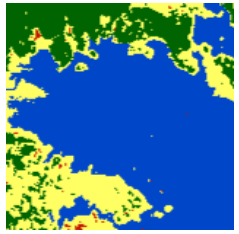

Water Body

Based on model's classification results

LAND COVER **MAP**

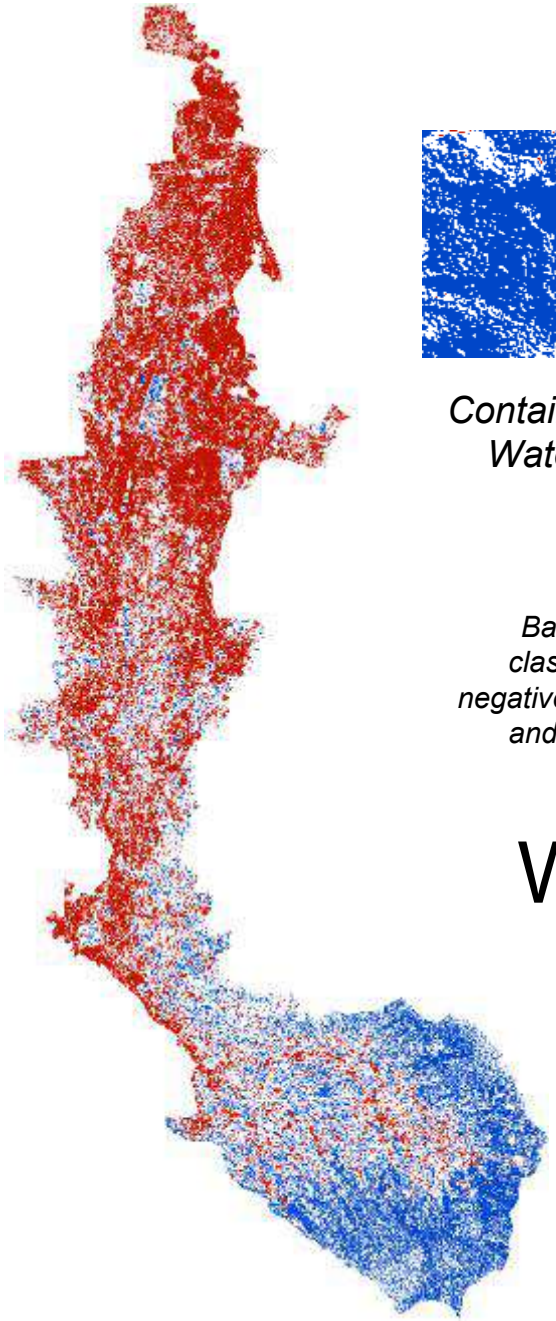

Containing Water

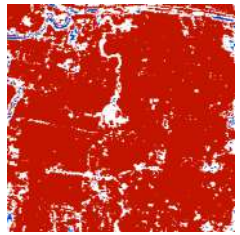

Not Containing Water

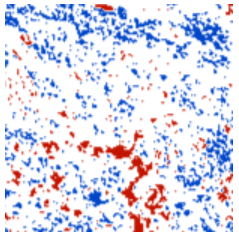

Not Strong Enough to be Classified as Containing Water

Based on LSWI value calculations, values above 0.2 are classified as water-saturated and therefore contain water, negative values do not contain water, while values between 0 and 0.2 are classified as having low water content but not saturated enough to be classified as water-saturated.

WATER CONTENT ESTIMATION **MAP**

CISARUA (Land Cover Mapping)

The First Segment – DAS CILIWUNG

2019

2021

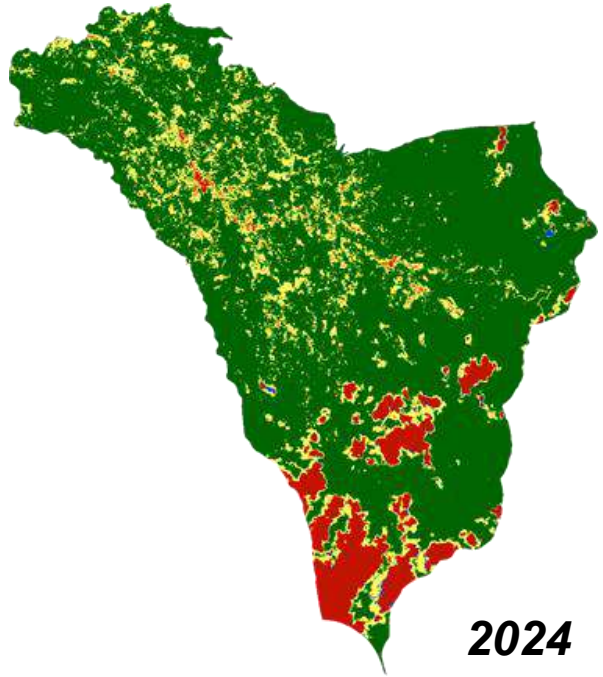

2024

CISARUA (Infiltration Estimation)

The First Segment – DAS CILIWUNG

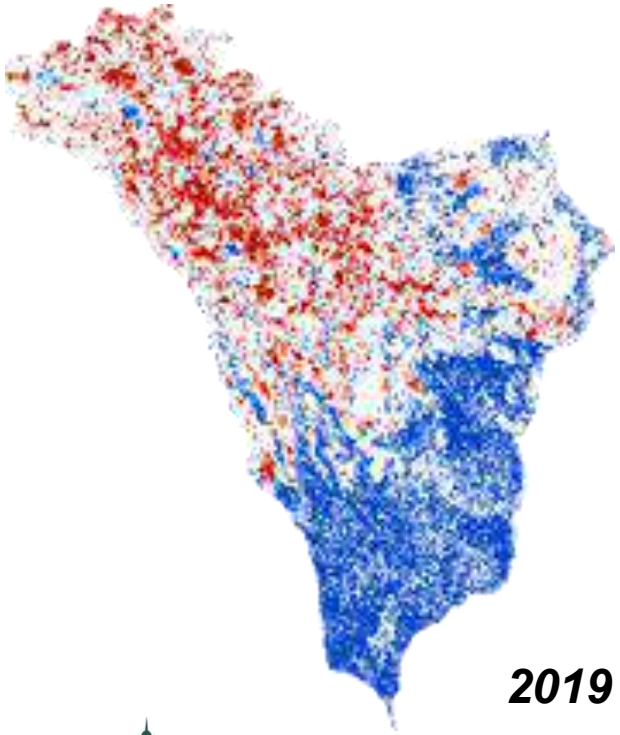

2019

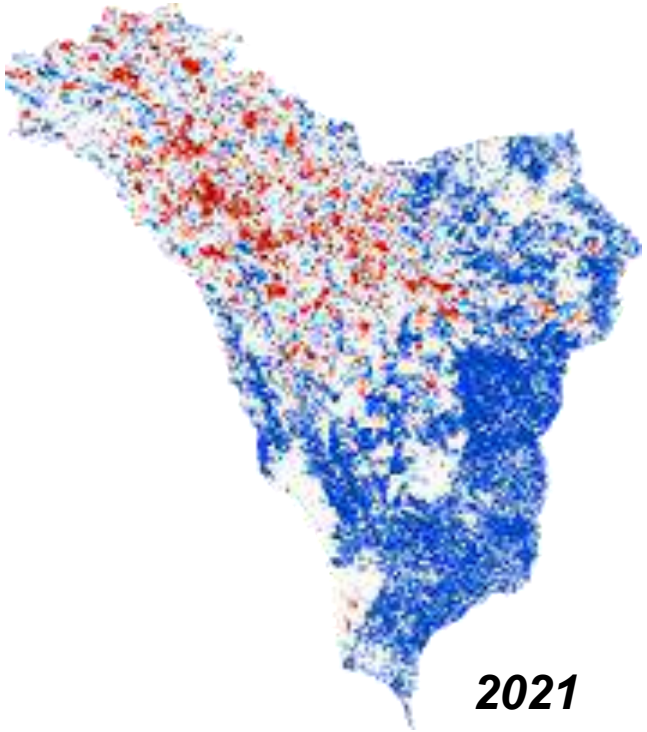

2021

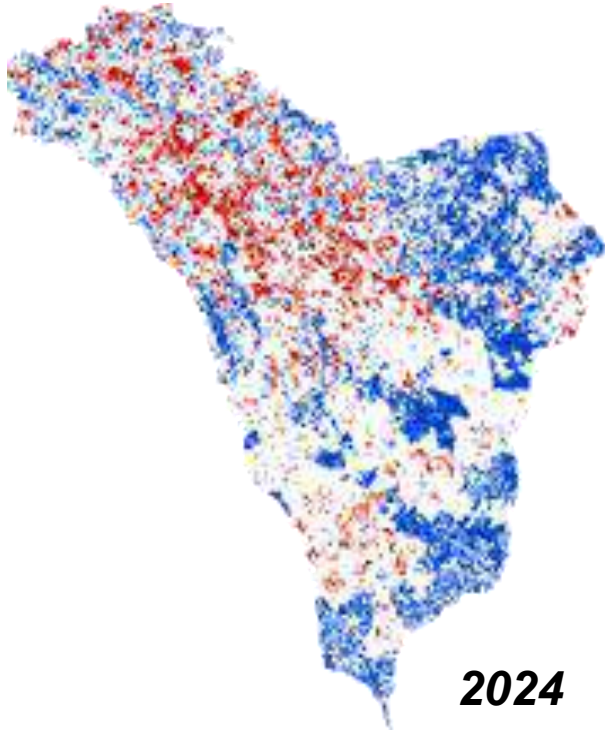

2024

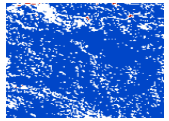

Containing Water

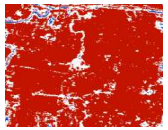

Not Containing Water

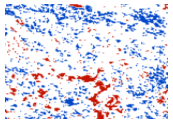

Not Strong Enough to be Classified as Containing Water

CIBINONG (Land Cover Mapping)

The Second Segment – DAS CILIWUNG

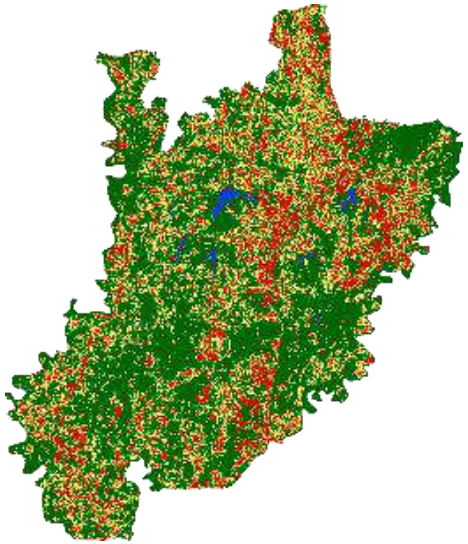

2019

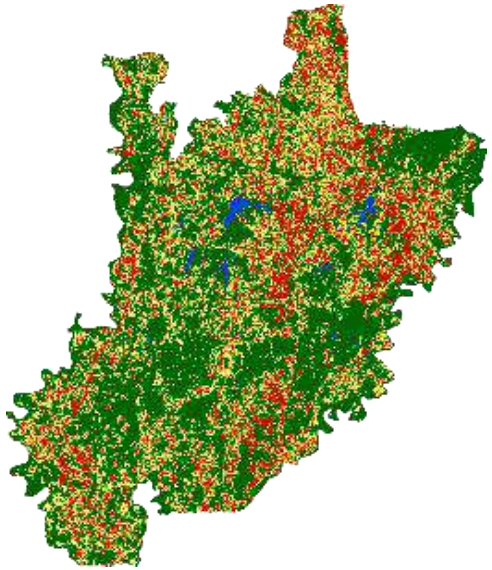

2021

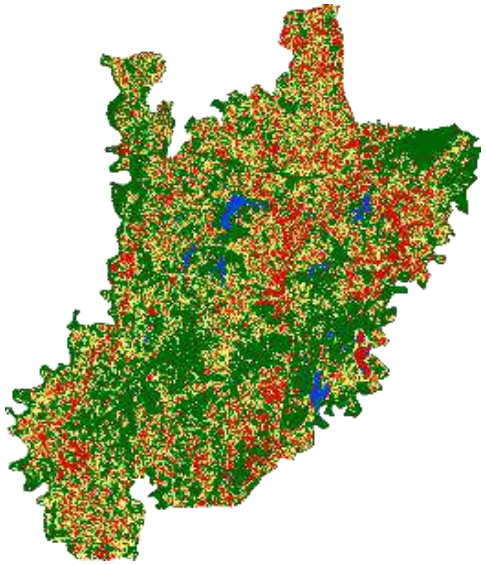

2024

CIBINONG (Infiltration Estimation)

The Second Segment – DAS CILIWUNG

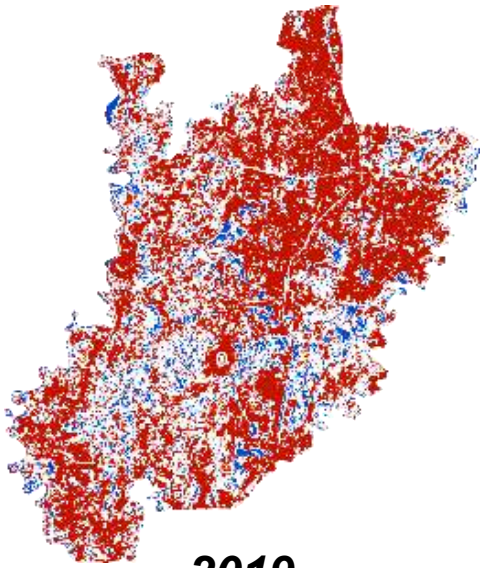

2019

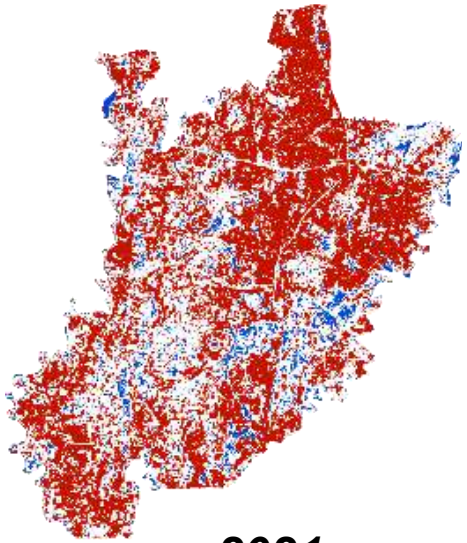

2021

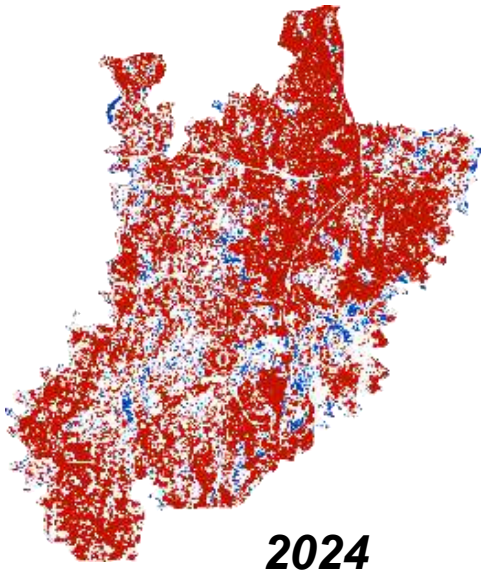

2024

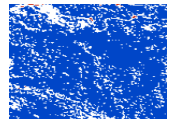

Containing Water

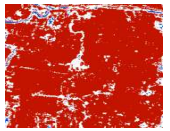

Not Containing Water

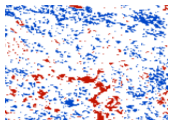

Not Strong Enough to be Classified as Containing Water

BOJONG GEDE (Land Cover Mapping)

The Third Segment – DAS CILIWUNG

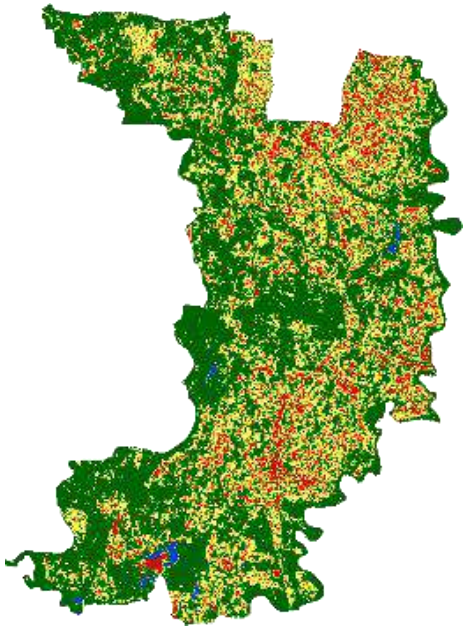

2019

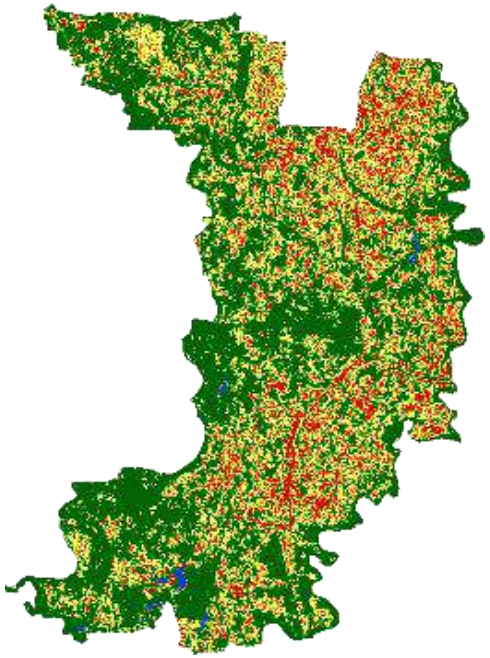

2021

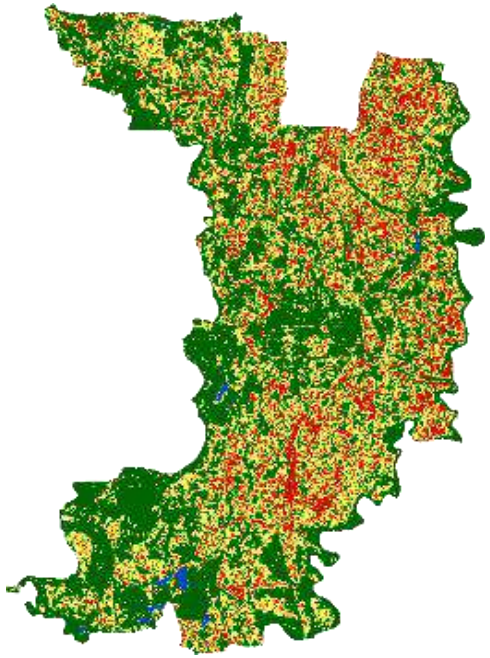

2024

BOJONG GEDE (Infiltration Estimation)

The Third Segment – DAS CILIWUNG

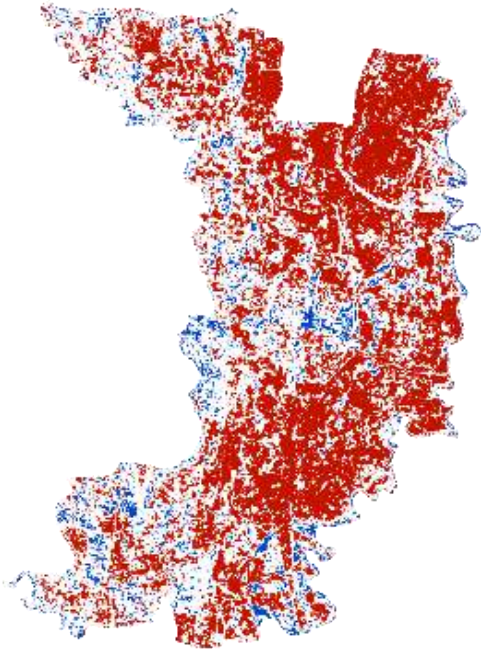

2019

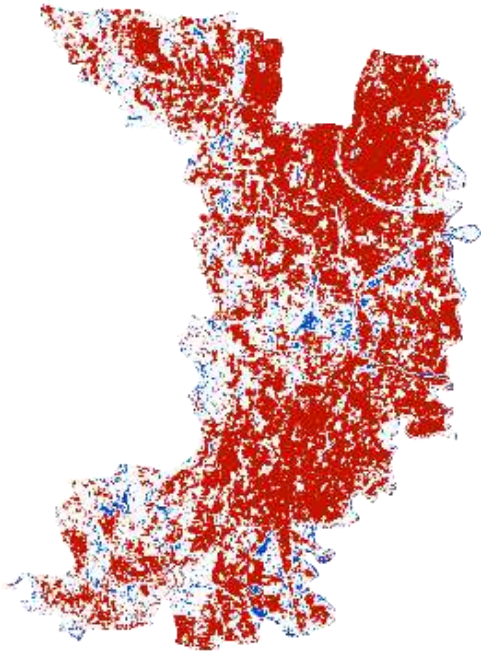

2021

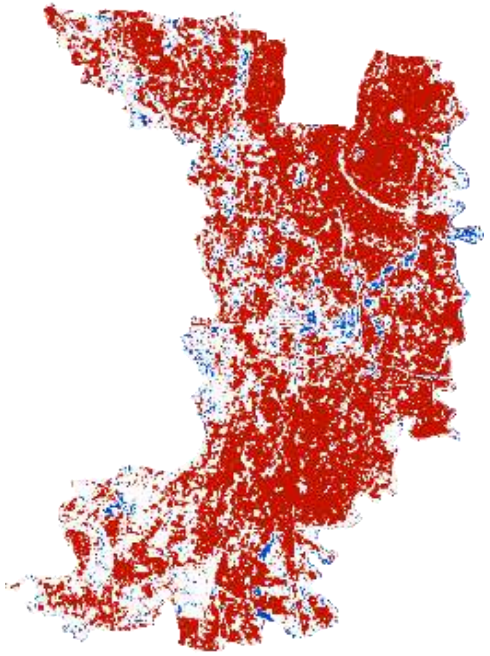

2024

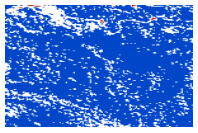

Containing Water

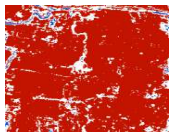

Not Containing Water

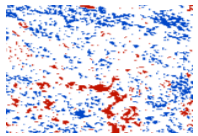

Not Strong Enough to be Classified as Containing Water

BEJI (Land Cover Mapping)

The Fourth Segment – DAS CILIWUNG

2019

2021

2024

BEJI (Infiltration Estimation)

The Fourth Segment – DAS CILIWUNG

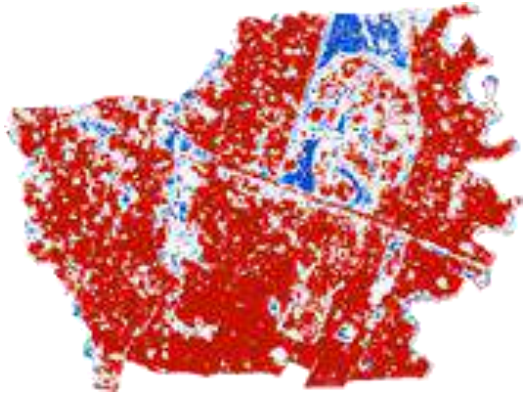

2019

2021

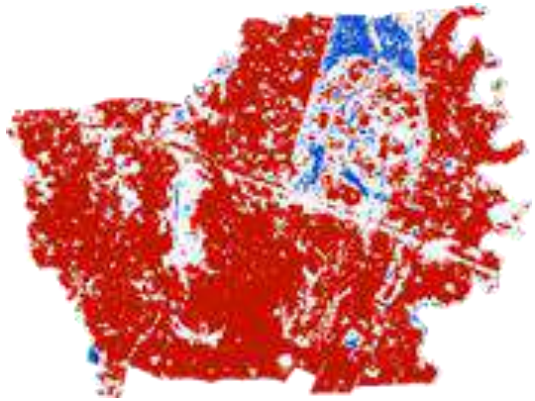

2024

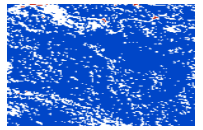

Containing Water

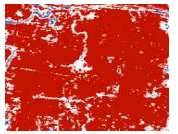

Not Containing Water

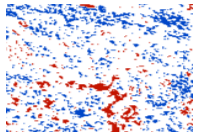

Not Strong Enough to be Classified as Containing Water

JAGAKARSA (Land Cover Mapping)

The Fifth Segment– DAS CILIWUNG

2019

2021

2024

JAGAKARSA (Infiltration Estimation)

The Fifth Segment– DAS CILIWUNG

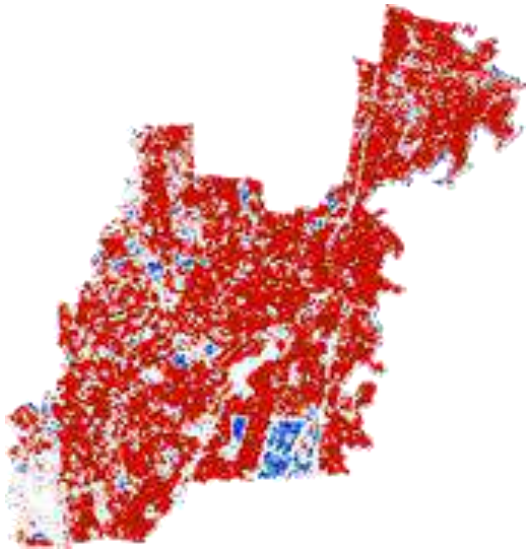

2019

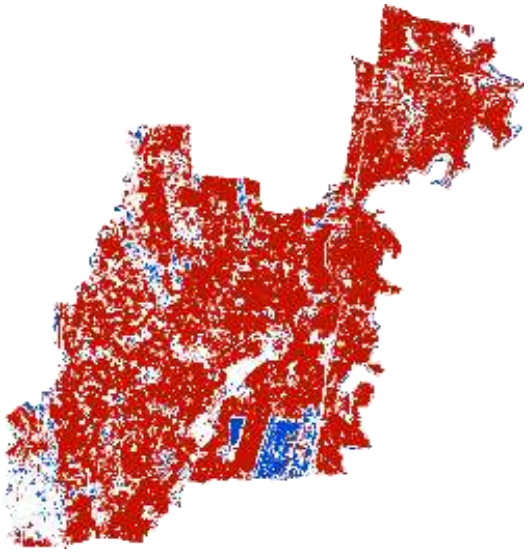

2021

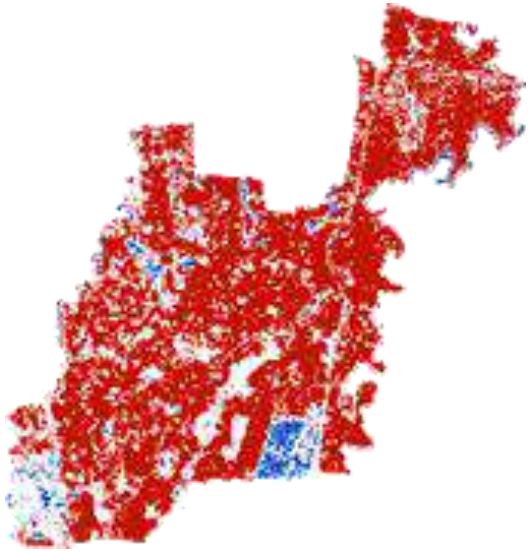

2024

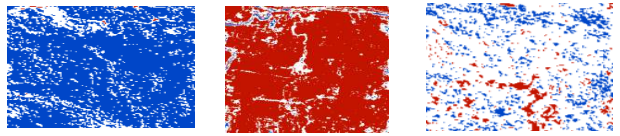

Containing Water

Not Containing Water

Not Strong Enough to be Classified as Containing Water

MENTENG (Land Cover Mapping)

The Sixth Segment– DAS CILIWUNG

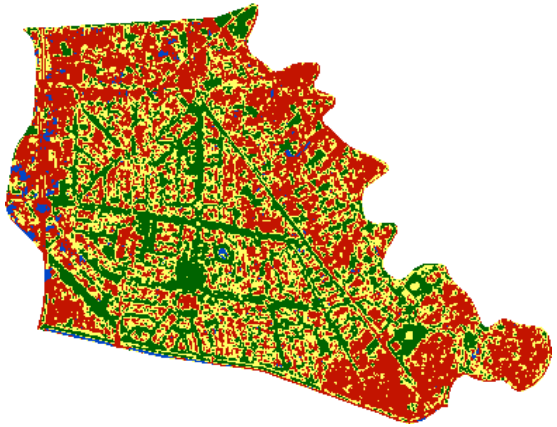

2019

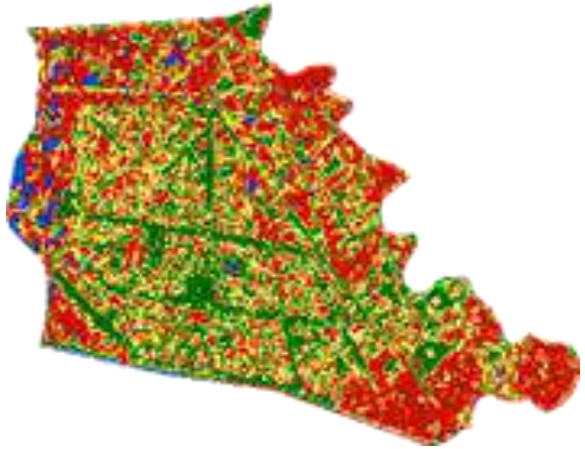

2021

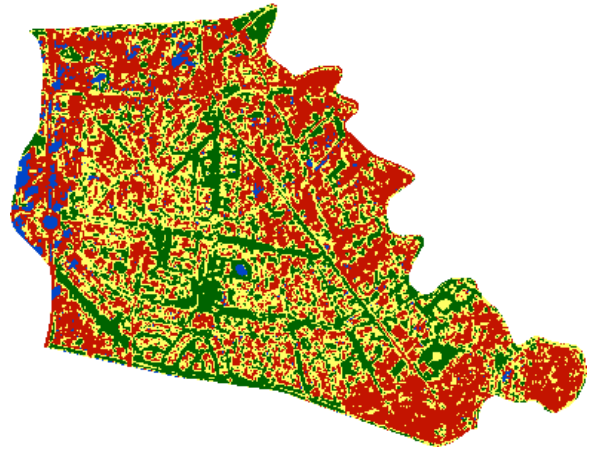

2024

MENTENG (Infiltration Estimation)

The Sixth Segment– DAS CILIWUNG

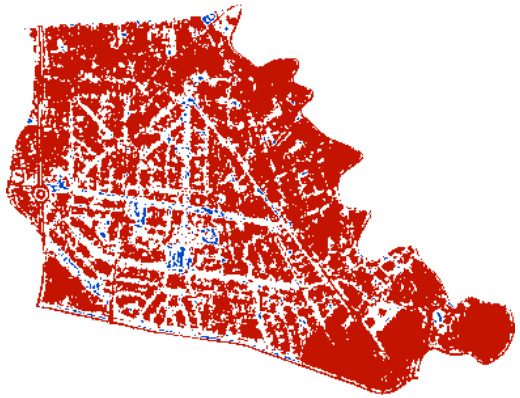

2019

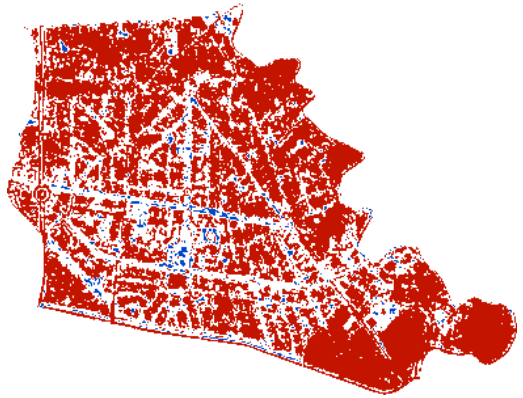

2021

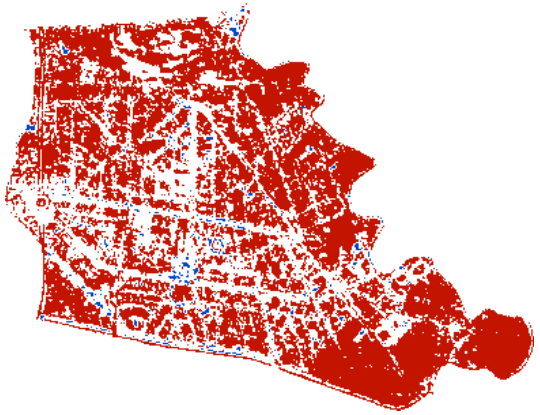

2024

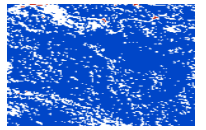

Containing Water

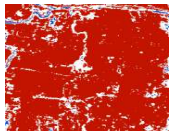

Not Containing Water

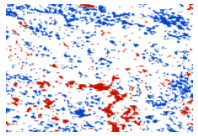

Not Strong Enough to be Classified as Containing Water

Ciliwung River Flow (Land Cover Mapping)

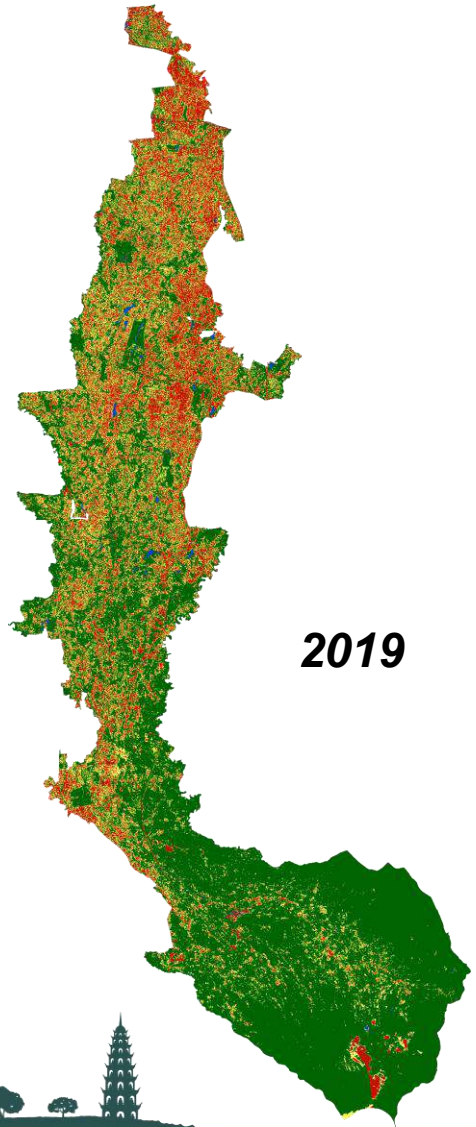

2019

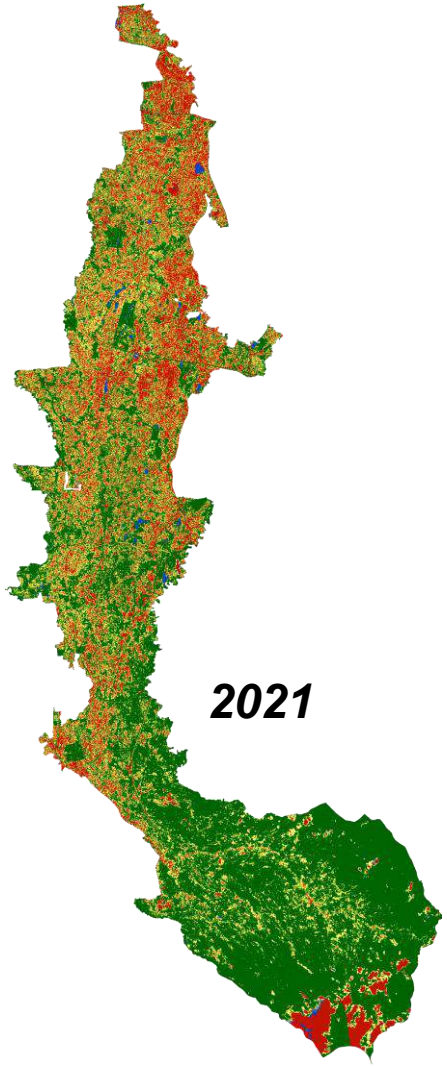

2021

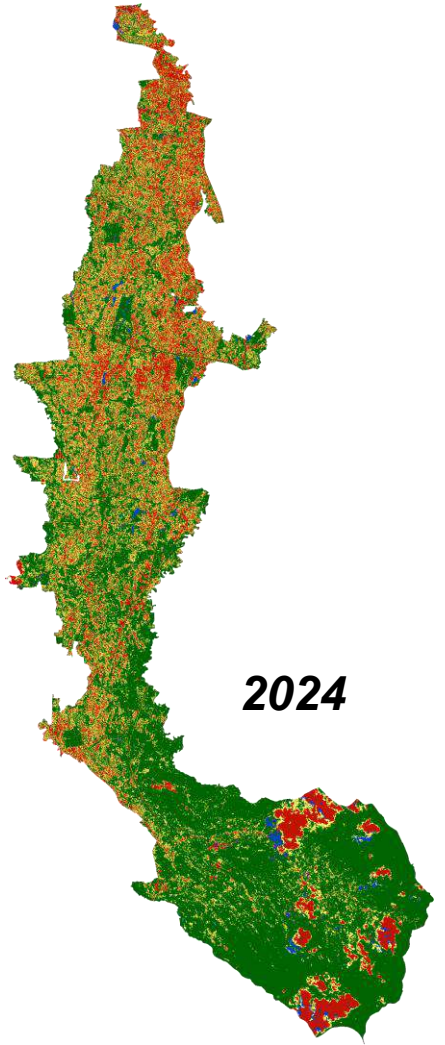

2024

Ciliwung Riverflow (Infiltration Estimation)

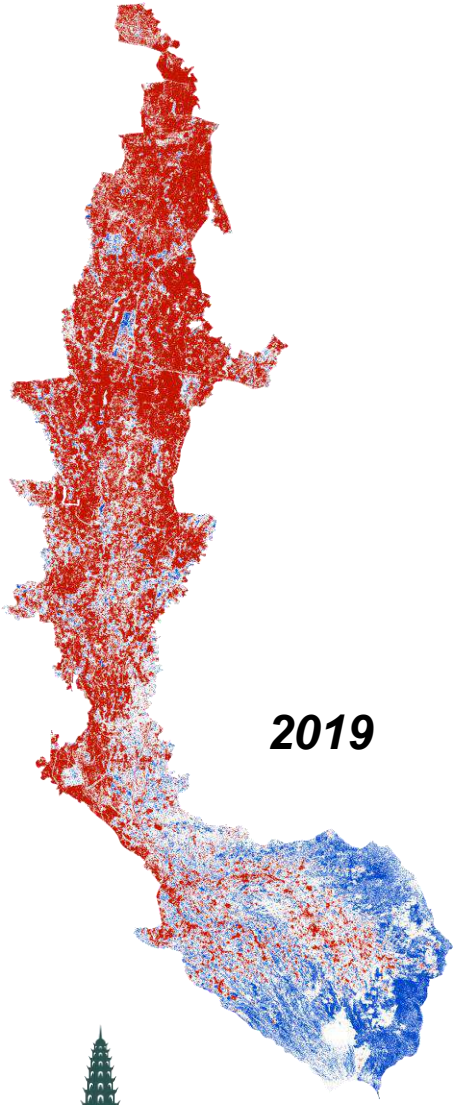

2019

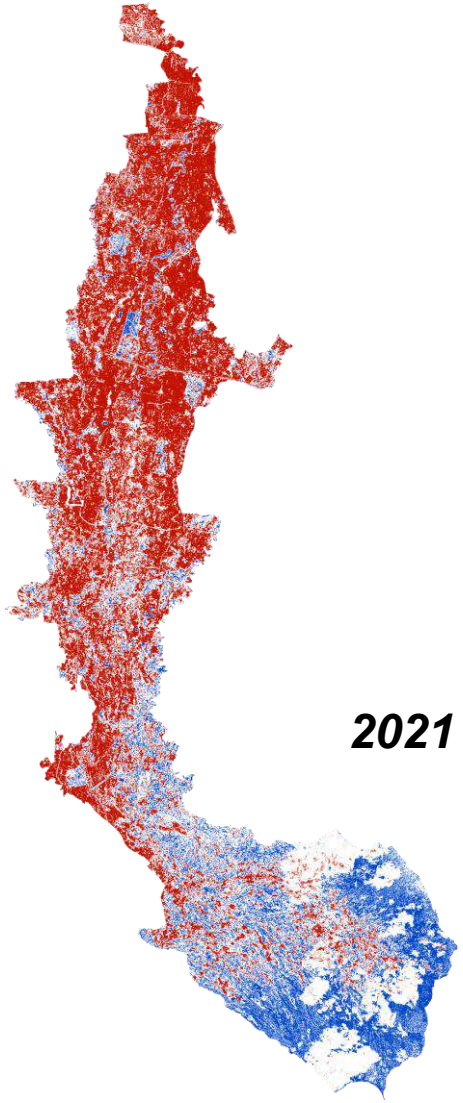

2021

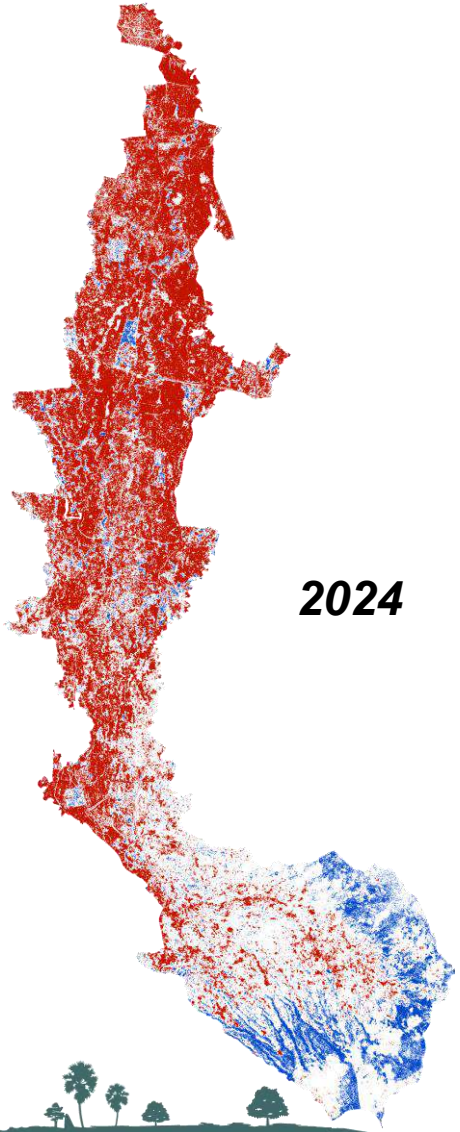

2024

Mapping Results – Cisarua

The First Segment – DAS CILIWUNG

Land Cover Class	2018		2020		2022		2024	
	Area (km²)	Infiltration Estimated	Area (km²)	Infiltration Estimated	Area (km²)	Infiltration Estimated	Area (km²)	Infiltration Estimated
Pervious	62.6534	28.86%	61.9596	38.26%	54.0076	46.81%	55.1466	23.00%
Half-Pervious	6.0384	0.16%	6.1229	0.53%	7.8197	0.90%	10.0813	0.42%
Impervious	2.1279	0.01%	2.6542	0.20%	7.6776	0.22%	5.4865	0.07%
Water Body	0.2473	5.18%	0.3305	5.05%	1.5623	2.91%	0.3528	2.04%
Total Infiltration Estimated		**25.48%**		**33.43%**		**35.76%**		**17.92%**

Mapping Results – Beji

The Fourth Segment – DAS CILIWUNG

Land Cover Class	2018		2020		2022		2024	
	Area (km²)	Infiltration Estimated	Area (km²)	Infiltration Estimated	Area (km²)	Infiltration Estimated	Area (km²)	Infiltration Estimated
Pervious	6.4431	12.49%	5.9229	10.92%	5.876	13.72%	4.9153	12.10%
Half-Pervious	5.3548	0%	4.4425	0%	4.5713	0%	4.9067	0%
Impervious	2.6811	0%	4.0987	0%	3.999	0%	4.596	0%
Water Body	0.1493	0.07%	0.1642	0.30%	0.182	0.55%	0.2103	0.19%
Total Infiltration Estimated		**5.50%**		**4.42%**		**5.52%**		**4.07%**

The Environmental Impacts

- The rise of sea levels above the land along Jakarta's coastline highlights the significant risk of land subsidence and potential urban inundation.
- Land subsidence in Jakarta primarily results from excessive groundwater extraction for domestic, commercial, and industrial use. In North Jakarta, subsidence rates range from 11 to 12 centimeters per year, coinciding with an annual sea-level rise of 0.4 to 0.5 centimeters.

The Environmental Impacts

The Governor of Jakarta has proposed the construction of the National Capital Integrated Coastal Development (NCICD) embankment, a 28.2-kilometer tidal wall intended to protect the coastline from tidal flooding.

2026 The 10th International Conference on Green Energy and Applications (ICGEA 2026)

March 6-8, 2026 |Hanoi, Vietnam

Invitation Letter

Dear Prof. Dyah Erny Herwindiati,

Thanks for your contribution!

We are pleased to announce that **2026 The 10th International Conference on Green Energy and Applications** (ICGEA 2026) will be held at **Hanoi, Vietnam** on **March 6-8, 2026**, which is sponsored by Hanoi University of Science and Technology, Hanoi, Vietnam. For more information, please visit our official conference website:www.icgea.org.

On behalf of the Organizing Committee, it is with great pleasure and sincere admiration for your distinguished expertise, extensive experience, and outstanding achievements in the field that we extend to you an invitation to join our conference as an **Invited Speaker**. Given your internationally recognized contributions, we are confident that your participation would greatly enrich this event. We sincerely hope that you might be able to accommodate this engagement within your busy schedule.

The conference is addressed to academics, researchers and professionals with a particular interest related to the conference topic. It brings together academics, researchers and professionals in the field of **Green Energy and Applications** making the conference a perfect platform to share experience, foster collaborations across industry and academia, and evaluate emerging technologies across the globe.

We sincerely invite you to attend the conference and actively engage in academic exchanges with fellow researchers and experts. Your participation will undoubtedly enrich the discussions and foster collaboration within the community.

We're looking forward to meeting you in ICGEA 2026!

ICGEA 2026
Conference Committee

Email: icgea_secretary@163.com
Tel: (00) 1 6193091099 (EN


2026 The 10th International Conference on
GREEN ENERGY
AND APPLICATIONS
IEEE
MRS

10th —— icgea.org

ICGEA 2026

INTERNATIONAL CONFERENCE ON GREEN ENERGY AND APPLICATIONS

March 6-8, 2026 | Hanoi, Vietnam

Call for Tracks

We invite proposals for specialized tracks/workshops to be held at ICGEA. Tracks should focus on emerging topics in Green Energy and Applications and provide a forum for in-depth discussions. Submit proposals to icgea_secretary@163.com.

Call for Tracks

Call for Nominations
ICGEA seeks nominations for Invited Talks. We welcome suggestions for distinguished researchers or practitioners who can address cutting-edge themes in Green Energy and Applications.
Please send nominations to *icgea_secretary@163.com.*

Topics (include but not limit)

Track 1: Renewable Energy Generation
- Solar and Photovoltaic Systems
- Wind Energy Conversion Technologies
- Biomass and Waste-to-Energy Systems
- Hydro and Ocean Energy
- Geothermal Energy Applications

Track 2: Energy Storage and Conversion
- Battery Technologies and Applications
- Hydrogen Energy and Fuel Cells
- Supercapacitors and Hybrid Storage Systems
- Power-to-Gas and Energy Conversion
- Thermal and Mechanical Energy Storage

Track 3: Smart Grids and Power System
- Smart Grids and Microgrids
- Integration of Renewable Energy into Power Grids
- Power System Operation, Stability, and Control
- Energy Management and Demand Response
- Power System Protection and Resilience

Track 4: Electrification and Sustainable Transportation
- Electric Vehicles and Charging Infrastructure
- Vehicle-to-Grid (V2G) and Grid Support
- Hydrogen-powered Mobility
- Power Electronics for Transportation
- Green Logistics and Low-emission Transport

Track 5: Digitalization and Intelligence in Energy Systems
- Artificial Intelligence in Power and Energy Systems
- Energy Forecasting with Big Data Analytics
- Internet of Things (IoT) for Smart Energy
- Digital Twin Technologies in Energy Applications
- Blockchain and Secure Energy Transactions

Track 6: Low-carbon Technologies and Sustainable Development
- Carbon Capture, Utilization and Storage (CCUS)
- Low-carbon Hydrogen Production Technologies
- Energy Policy, Markets, and Regulatory Frameworks
- Climate-resilient Energy Systems
- Green Building and Zero-energy Communities

For more topics, please visit: h*ttp://www.icgea.org/topics.html*

Important Date

Submission Deadline
February 1, 2026

IEEE

Sponsored by

Patrons

Publication

IEEE

Submitted papers will be reviewed by Technical Program Committee and sub-review-ers.All accepted papers after proper presentation and registration will be collected in IEEE conference proceedings, which will be included in IEEE Xplore and indexed by EI Compendex and Scopus, etc.

***Proceedings of ICGEA 2017-2025 have already been included in IEEE Xplore, indexed by Scopus and EI Compendex!**

Submission Guideline

1.Full paper (Presentation & Publication)
2.Abstract (Presentation only)
Submission Link: *http://confsys.iconf.org/submission/icgea2026*
Email submission: *icgea_secretary@163.com or icgea@young.ac.cn*

ICGEA will accept full paper (publication) or abstract (presentation only) submission, the full paper should match the template requirements. Or you can register as a listener to attend.

Committee

Conference Chairs
Siew Hwa Chan, Nanyang Technological University, Singapore
King Jet TSENG, Singapore Institute of Technology, Singapore, IEEE FELLOW
Huynh Quyet Thang, President of Hanoi University of Science and Technology, Vietnam, IEEE Member

Conference Co-Chairs
Yiyan Pei, Singapore Institute of Electronics, Singapore
Igor Kuzle, University of Zagreb, Croatia

Program Chairs
Jianping Yang, Central South University, China
Nguyễn Hữu Thanh, Hanoi University of Science and Technology, Vietnam, IEEE Member

Local Chairs
Hoàng Sĩ Hồng, Hanoi University of Science and Technology, Vietnam
Đinh Văn Hải, Hanoi University of Science and Technology, Vietnam

Regional Chairs
Thaiyal Naayagi Ramasamy, Newcastle University, Singapore, IEEE Senior Member
Anurag Sharma, Newcastle University in Singapore, IEEE Senior Member
Dhivya Sampath Kumar, Singapore Institute of Technology, Singapore, IEEE Senior Member
Sunil Kumar Dube, Senior Power Electronics Engineer, California, United States
Salish Maharjan, Iowa State University, United States

Publicity Chairs
Tuyen Nguyen Duc, Hanoi University of Science and Technology, Vietnam
Viboon Sricharoenchaikul, Chulalongkorn University, Thailand
Weeratunge Malalasekera, Loughborough University, United Kingdom
Publication Chair

Treasurer
Jack Bennett, Lincoln University, New Zealand

Chairman of Communications
Nguyen Duc Tuyen, Hanoi University of Science and Technology, Vietnam

History

ICGEA 2017 | IEEE | ISBN:978-1-5386-3984-9 | Scopus & EI Compendex
ICGEA 2018 | IEEE | ISBN:978-1-5386-5234-3 | Scopus & EI Compendex
ICGEA 2019 | IEEE | ISBN:978-1-7281-1382-1 | Scopus & EI Compendex
ICGEA 2020 | IEEE | ISBN:978-1-7281-6020-7 | Scopus & EI Compendex
ICGEA 2021 | IEEE | ISBN:978-1-7281-7715-1 | Scopus & EI Compendex
ICGEA 2022 | IEEE | ISBN:978-1-6654-2051-8 | Scopus & EI Compendex
ICGEA 2023 | IEEE | ISBN:978-1-6654-5609-8 | Scopus & EI Compendex
ICGEA 2024 | IEEE | ISBN:979-8-3503-4900-9 | Scopus & EI Compendex
ICGEA 2025 | IEEE | ISBN:979-8-3315-3077-8 | Scopus & EI Compendex

Contact Us

Evelyn Koh
icgea_secretary@163.com
Tel: +86-134-0855-5552(Chinese) +001-6193091099(English)

Invited Speakers

Professor. Li Sun,

Southeast University, China

Li Sun, IEEE Senior Member, received the PhD degree from Tsinghua University in 2017. He is currently the Youth Chair Professor in the School of Energy and Environment at Southeast University, Nanjing, China. He was a Visiting Associate Professor in Cornell University since 2019 to 2020. He is mainly engaged in the research of dynamics and control of energy systems with thermal and hydrogen components. He has led over 30 national and enterprise commissioned research projects with more than 20 million CNY, and authored 1 book and more than 120 referred journal papers with more than 5000 citations. He was listed in the Stanford's top 2% top scientists in the world. He is the Chair of IFAC TC 6.3A on Power Systems and Power Electronics and Vice Chair of the Working Group of IEEE Standard P3464 and (guest) editors of renowned journals like Energy, Renewable Energy, and Control Engineering Practice. He is appointed as the Publishing Ethics Advisor for Elsevier in 2026. He was awarded the National-level Youth Talent Fellowship of China in 2023 and Jiangsu Province Outstanding Young Scholars Fund in 2024. As the leading scientist, he won the First Prize of China Electric Power Science and Technology Award and the Second Prize of Jiangsu Province Science and Technology Progress Award, for contributions to the coordinated control of electricity and heat integrated energy systems.

Title: The Role of Thermal Inertia in Improving the Flexibility of Power Grid with High Renewable Penetration

Abstract: Thermal inertia widely exists in the power systems, such as the thermal power generation in the source side and the heat pump applications in the load side. These thermal inertia is usually caused by the slow dynamics of the temperature and pressure of working fluid such as water/steam, air or refrigerant within a limited volume. This talk will discuss the potential of utilizing the thermal inertia to help smooth the fluctuation of renewable energy and thus improve the flexibility of the power grid. However, the inertia of different thermal components exhibit different time-scale dynamics and requires cautious control design. This talk begins with the dynamic modelling and analysis methods. Several uncertainty compensation based control methods are proposed for different thermal processes, including Economic Model Predictive Control (EMPC) for the energy efficiency optimization of multivariable processes. To demonstrate the efficacy, some field applications of thermal inertia control are introduced in the cases like coal-fired power plant, building energy systems and cascaded heat pump systems for distributed steam generation in industry.

Professor. Dyah Erny Herwindiati,

Universitas Tarumanagara, Indonesia

Dyah Erny Herwindiati has been a Professor of Informatics Engineering at Tarumanagara University since 2014. She received her doctorate in Mathematics from the Bandung Institute of Technology (ITB) in 2006, where she wrote her dissertation on "A New Criterion of Robust Estimation for Location and Covariance Matrix and Its Application in Outlier Labeling." Dyah also serves as the Dean of the Faculty of Information Technology at Tarumanagara University in Jakarta, a role she has held since 2014 and will continue until 2026.

After completing her doctorate, she developed algorithms for processing satellite imagery and remote sensing data. Her contributions have enhanced the accuracy of data analysis across multiple fields.

She has worked as a Visiting Researcher in the Mathematics Department at the Conservatoire National des Arts et Métiers (CNAM) University in France and at Universiti Teknologi Malaysia (UTM) in Malaysia. Minister of Education Indonesia has recognized her expertise and contributions in Data Science by officially appointing her as a Full Professor. Her research has made a strong impact in several areas, especially in Machine Learning.

Title: Decline in Water Infiltration in the Ciliwung River Flow: Applications of Machine Learning and Environmental Impacts

Abstract: The Ciliwung River is a principal waterway in the Jakarta metropolitan area, extending approximately 124.1 km and encompassing a catchment area of about 370.8 km2. It serves as a critical water source for both West Java and Jakarta. Originating in the mountainous

regions of Bogor Regency, such as Mount Gede, Pangrango, and Cisarua, the river flows northward to Jakarta Bay in the Java Sea. The Ciliwung River provides essential ecological and social services, including raw water supply, biodiversity support, and surface water flow regulation, highlighting its significance for regional sustainability.

Jakarta, Indonesia's economic and business center, has experienced substantial in-migration and rapid urbanization. By 2019, the population density reached 16,704 people per square kilometer, significantly surpassing the national average of 141.

The high cost of living in Jakarta has prompted many migrants to settle in surrounding buffer cities, with Bogor serving as a primary destination. Once characterized by its watershed and extensive green spaces, Bogor has experienced significant urban transformation. Consequently, the Ciliwung River, which originates in Bogor and flows through Depok, has been adversely affected by ongoing urbanization.

Intensive urbanization has converted sub-districts along the Ciliwung River from green spaces into built-up, impervious areas. This land-use change has reduced the region's water-catchment capacity and its ability to absorb and retain water, resulting in a significant decline in infiltration. The shift from pervious to impervious land cover presents considerable environmental challenges.

Decreased infiltration into the Ciliwung River has reduced the availability of clean water. This decline has led to increased groundwater extraction for domestic, commercial, and industrial use in Jakarta, resulting in significant land subsidence. Consequently, sea levels now exceed the land surface in some locations. In certain areas of Jakarta, land is subsiding by up to 11 cm per year, a rate much higher than global sea-level rise.

This research aims to analyze annual land cover changes in the Ciliwung River flow by classifying pervious, semi-pervious, impervious, and water body surfaces using Sentinel-2 satellite imagery. Additionally, it investigates the spatial and temporal distribution of infiltration across multiple sub-districts within the Ciliwung River area, utilizing land-cover mapping and data preparation to support subsequent machine learning modelling.

The study utilizes Copernicus Sentinel-2 Collection 1, equipped with the MultiSpectral Instrument Level-2A (MSI L2A), which provides satellite imagery across 13 spectral bands. These data are atmospherically corrected and require no further radiometric adjustment. The 10-meter spatial resolution constrains the detection of finer features. Sentinel-2 revisits the study area every five days.

Kernel Ridge Regression is an extension of Ridge Regression that incorporates L2 regularization to address multicollinearity in the data. By applying the kernel trick, data are mapped to a higher-dimensional feature space, enabling the capture of both linear and non-linear correlations. In this study, Kernel Ridge Regression is used to train classification models with ten predictor variables derived from Sentinel-2 spectral bands.

Model evaluation results indicate a precision of 97.42%, a recall of 97.39%, and an F1-score of 97.4%. These metrics demonstrate the

model’s effectiveness in classifying data into predefined categories. The classification results were compared with true- and false-color composites to assess accuracy under actual field conditions. The comparison confirms that the model can distinguish between green land, built-up land, and water bodies.

Professor. Jinlong Ma,

APEC Sustainable Energy Center, Tianjin University , China

Jinlong Ma is a Professor at Tianjin University, China, and Vice President of APEC Sustainable Energy Center (APSEC). At APSEC, he is responsible for advisory and research programs; one of the main current research themes concerns energy transition solutions in APEC economies. Prior to the current role, Dr. Ma worked in many Asia and Pacific countries and held senior positions at renowned academic and research institutions, technical and advisory service organizations, and international energy corporations. His areas of expertise include energy system planning, renewables, power sector development, electricity market analysis, energy conservation and efficiency, urban energy, greenhouse gas inventory and emission abatement strategies. Jinlong holds a PhD in Energy Economics from the University of Melbourne, an M.Eng. in Energy Policy and Planning from the Asian Institute of Technology, and a B.Eng. in Electrical Engineering from North China University of Electric Power. He serves as a Fellow of the Australian Institute of Energy (AIE), is a member of International Association of Energy Economics (IAEE) and the Institute of Electrical and Electronics Engineers (IEEE).

Title: Supporting green energy transition in medium- and small-sized towns

Abstract: The urbanization in counties is the driver of national demographic changes and is a salient characteristic of the China's social and economic environment. Counties are in the primary position in the urbanization process, and with carbon emissions at the county-level accounting for more than 60% of national total in China, and a large proportion of counties' economic activities, energy consumption, and carbon emission occur in SMTs, which places counties at the crux of the national green energy transition strategies. Promoting the transition toward clean energy in counties is crucial for achieving the national dual carbon goals. As an important link between rural areas and cities, the urban areas of counties, i.e., small and medium-sized towns (SMTs), are pivotal in defining the new urbanization trend, and implementing the national rural revitalization strategy. This presentation outlines a research initiative designed to facilitate the advancement of low-carbon energy systems within SMTs in China. The program encompasses the identification of country-specific characteristics, the selection of pilot projects, a thorough evaluation of the current energy infrastructure, and the optimization of energy systems to achieve low-carbon objectives. Accompanied by targeted policy recommendations, this research seeks to serve as a reference for ongoing energy transition initiatives in the counties in China, as well as in comparable administrative divisions across other developing nations in Asia and the Pacific.

Asst. Prof. Trang Nakamoto,

Ritsumeikan University, Japan

Trang Nakamoto, born in Vietnam in 1986, is an assistant professor at Ritsumeikan University. He earned his B.Eng. from Hanoi University of Science and Technology in Vietnam (2009), followed by a Master's degree from Dongguk University in South Korea (2011) and a Ph.D. from Ritsumeikan University in Japan (2014). After two years working in industry, he returned to academia in 2017 as a senior researcher at R-

GIRO. His research focuses on the development of innovative biosensors powered by microbial fuel cell (MFC) technology. He is recognized for pioneering practical, low-cost MFC-based biosensors for critical applications in environmental monitoring and smart agriculture. With over 40 peer-reviewed publications and more than 50 international conference presentations, contributing significantly to the advancement of bio-electrochemical sensing technologies.

Title:Harnessing Microbial Fuel Cells for Biosensing Applications and Green Energy

Abstract: Microbial Fuel Cells (MFCs) offer a unique platform for both green energy generation and, more powerfully, self-powered biosensing. This presentation introduces advanced MFC-based biosensing technologies and highlights our research advancements in transforming microbial bio-electrochemistry into real-time, actionable data for environmental and agricultural monitoring, overcoming the cost and power limitations of traditional sensors.

Our research focuses on developing practical, MFC-based biosensors that leverage microbial metabolism to detect environmental changes. We will present case studies including floating sensors for tracking organic pollution in wastewater and portable devices for sensing soil water content in smart agriculture. A cornerstone of our work is sustainability; we have pioneered novel, low-cost electrodes derived from waste biomass like rice husks and loofah sponges. While these devices are powered by the green energy they generate from waste, their primary value lies in their function as autonomous sensors. Our work demonstrates a clear pathway toward developing intelligent, sustainable sensor networks for a smarter, greener future.

Dr. Shitikantha Dash,

National University of Singapore, Singapore

I am a post-doctoral research fellow at the National University of Singapore (NUS), Singapore. Here, I am working with Prof. Dipti Srinivasan's research group towards developing Singapore's largest V2G testbed. Prior to this, I worked as a research associate at the Indian Institute of Technology (IIT) Ropar, Rupnagar, India, under a CRG project sponsored by the Science and Engineering Research Board (SERB), New Delhi.

I completed my bachelor's at the Biju Patnaik University of Technology (BPUT), Odisha, India, in Electrical and Electronics Engineering, and my master's at the Center for Advanced Post Graduate Studies, BPUT, Rourkela, India, in Power System Engineering. Then I moved to the Indian Institute of Technology Ropar, Rupnagar, India, for my PhD program in the Department of Electrical Engineering under the supervision of Prof. Ranjana Sodhi from the EE department and Prof. Balwinder Sodhi from the CS department.

My primary research interest includes demand response, energy market, energy storage systems, distributed energy resources management, and residential load monitoring. When I am not doing research, you may find me at the pool table in staff launge. I also enjoy post-independence Odia literature and editing Odia Wikipedia.

Title: Profit-Aware EV Utilisation Model for Sustainable Smart Cities: Joint Optimisation over EV System, Power Grid System, and City Road Grid System

Abstract: A sustainable city requires a sustainable means of transportation. This ambition is leading towards higher penetration of electric vehicles (EVs) in our cities, in both the private and commercial sectors, putting an ever greater burden on the existing power grid. Modern deregulated power grids vary electricity tariffs from location to location and from time to time to compensate for any additional burden. In this paper, we propose a profit-aware solution to strategically manage the movements of EVs in the city to support the grid while exploiting these locational, time-varying prices. This work is divided into three parts: (M1) profit-aware charging location and optimal route selection, (M2) profit-aware charging and discharging location and optimal route selection, and (M2b) profit-aware charging and discharging location and optimal route selection considering demand-side flexibility. This work is tested on the MATLAB programming platform using the Gurobi optimisation solver. From the extensive case studies, it is found that M1 can yield profits up to 2 times greater than those of its competitors, whereas M2 can achieve profits up to 2.5 times higher and simultaneously provide substantial grid support. Additionally, the M2b extension makes M2 more efficient in terms of grid support.

Dr. Lintong Liu,

CNOOC Energy Economics Institute, China

Title: Technical Pathways, Cost-Effectiveness, and Policy Mechanisms of Sustainable Aviation Fuel: A Comprehensive Assessment of Singapore's Experience

Abstract: Against the backdrop of global energy transition and carbon neutrality goals, the aviation industry has emerged as a critical sector for emissions reduction due to its high energy consumption and carbon intensity. Sustainable Aviation Fuel (SAF) has gained increasing attention as a key decarbonization pathway in aviation, owing to its significant lifecycle emissions reduction potential and compatibility with existing infrastructure. As a global aviation hub, Singapore has made remarkable progress in SAF development by integrating policy support, technological deployment, and market mechanisms. This paper systematically reviews the current state of SAF in Singapore, analyzing its industry layout, technological pathways, policy design, and international cooperation. A comparative analysis is conducted to draw implications for China's SAF development. The study finds that China can accelerate SAF industrialization and enhance international competitiveness by optimizing policy frameworks, upgrading technology systems, and deepening regional collaboration, thereby supporting

its broader net-zero aviation goals. This paper combines a systematic literature review and case-study analysis with lifecycle assessment (LCA) and techno-economic modelling to generate quantitative policy simulation results that inform decision-making on regional SAF scaling pathways.
